

The Search for the Missing Baryons at Low Redshift

Joel N. Bregman

Department of Astronomy, University of Michigan, Ann Arbor, Michigan 48109-1090; email: jbregman@umich.edu

Annu. Rev. Astron. Astrophys. 2007. 45:221–59

First published online as a Review in Advance on June 20, 2007.

The *Annual Review of Astronomy and Astrophysics* is online at astro.annualreviews.org

This article's doi:
10.1146/annurev.astro.45.051806.110619

Copyright © 2007 by Annual Reviews.
All rights reserved

0066-4146/07/0922-0221\$20.00

Key Words

astrophysics, cosmology, intergalactic medium

Abstract

At low redshift, only about one-tenth of the known baryons lie in galaxies or the hot gas seen in galaxy clusters and groups. Models posit that these “missing baryons” are in gaseous form in overdense filaments that connect the much denser virialized groups and clusters. About 30% is cool ($<10^5$ K) and is detected in Ly α absorption studies, but about half is predicted to lie in the 10^5 – 10^7 K regime. Gas is detected in the 2 – 5×10^5 K range through OVI absorption studies (7% of the baryons) and possibly near 10^5 K from broad Ly α absorption (20% of the baryons). Hotter gas (0.5 – 2×10^6 K) is detected at zero redshift by OVII and OVIII K α X-ray absorption, and the OVII line strengths seem to correlate with the Galactic soft X-ray background, so it is probably produced by Galactic halo gas, rather than a Local Group medium. There are no compelling detections of the intergalactic hot gas (0.5 – 10×10^6 K) either in absorption or emission and these upper limits are consistent with theoretical models. Claimed X-ray absorption lines are not confirmed, while most of the claims of soft emission are attributable to artifacts of background subtraction and field-flattening. The missing baryons should become detectable with moderate improvements in instrumental sensitivity.

1. INTRODUCTION AND MOTIVATION OF THE ISSUES

In the past decade we have come to an appreciation of the “missing” baryon problem and the likely existence of a cosmologically important warm-hot intergalactic medium (WHIM) at low redshift. The belief was that the baryons at high redshift underwent gravitational collapse over cosmological time to become the galaxies present today. However, there was evidence of baryons not included in galaxies, such as the X-ray emitting gas in galaxy clusters, where the gas usually represented more baryons than those in the galaxies, but rich galaxy clusters are rare and galaxy groups do not possess a bright hot intergalactic medium. Also, the Ly α forest so prominent at high redshift is sparse near $z = 0$, so its contribution to baryons seemed small.

A stunning change occurred when a careful census of the baryons at low redshift was undertaken (Persic & Salucci 1992, Bristow & Phillipps 1994, Fukugita et al. 1998). The baryonic mass of galaxies appeared to be only one-tenth of the baryonic content at high redshift; this was a result first indicated by studies at least a decade earlier (see discussion in Persic & Salucci 1992). The mass at high redshift is measured from primordial nucleosynthesis and near $z = 3$ through the study of the Ly α lines, which measures the neutral gas content. This baryon content is confirmed to high accuracy with recent cosmic microwave background (CMB) studies, such as from the *Wilkinson Microwave Anisotropy Probe* (WMAP; Spergel et al. 2006), so it must be low redshift baryons that are missing. In quoting quantities, we use a flat Friedmann-Lemaître Λ CDM universe with $H_0 = 70 \text{ km s}^{-1} \text{ Mpc}^{-1}$, with $\Omega_\Lambda = 0.72$, $\Omega_{\text{DM}} = 0.23$, and $\Omega_{\text{baryon}} = 0.045$. For this universe, the mean baryon density is $4.2 \times 10^{-31} \text{ gm cm}^{-3}$, and for an ionized metal-free plasma, the mean particle density is $4.0 \times 10^{-7} \text{ cm}^{-3}$. The time since the Big Bang is 13.8 Gyr and the distance to a source at $z = 1$ is 3.35 Gpc.

In trying to account for the missing baryons, careful studies of the mass in galaxies, and in gaseous form in galaxy clusters, groups, and in the intergalactic medium were conducted. Since the first efforts in the late 1990s, there have been many observational campaigns to improve the numbers. We briefly discuss the updated census by Fukugita & Peebles (2004), which is consistent with other efforts (Shull 2003). For the census of the stellar content of galaxies, the availability of the Sloan Digital Sky Survey sample was of considerable help as it led to an improved understanding of the fraction of stars in spheroids compared to disks and to their M/L values (Kauffmann et al. 2003); a large number of low-luminosity galaxies is not a viable possibility for explaining the missing baryons. In estimating the stellar mass, there are a variety of assumptions, such as the shape of the initial mass function. Fukugita & Peebles (2004) assign uncertainties to these choices, leading to uncertainties of about 25% for the stellar content. Including white dwarfs, neutron stars, black holes, and substellar objects, along with the stars burning nuclear fuel, this component is about 6% of the total baryon rest mass. In quantifying the neutral gas content, recent surveys have greatly improved the accuracy of these numbers, such as the blind HI Parkes All Sky Survey (HIPASS) that includes 1000 galaxies (Zwaan et al. 2003). Such surveys show that the mass in neutral gas constitutes 1.7% of the baryon content, raising the total baryon content in galaxies to 7.7%. Thus, more than 90% of the baryons lie outside of galaxies, and this is known as the “missing” baryon problem.

Rich clusters of galaxies have several times more matter in gas than in galaxies. The X-ray emission from this hot gas has been used to determine its mass, and the baryon content of these rich clusters is consistent with the cosmological value (Allen et al. 2002). There are no missing baryons in rich clusters. However, only a few percent of the mass of the universe lies in rich clusters, so even though gas is abundant, it contributes only about 4% of the total baryon content. For decreasing cluster richness, down to galaxy groups, the ratio of the gas mass to the galaxy mass declines so that it is less than the mass of the galaxies. The difficulty with measuring the gaseous mass in rich clusters or in galaxy groups is that the baryon counting stops when the X-ray surface brightness falls below detectable levels, at about half of a virial radius for clusters and at smaller radii for most groups. In these outer parts of clusters and groups, the implied density is falling as r^{-p} , where $p = 1.5$ to 2 (Mulchaey 2000, Rasmussen & Ponman 2004), so the gaseous mass is still increasing at least linearly with radius at the last observable radius. Given this uncertainty, it is possible that a significant fraction of baryons lie in the outer parts of clusters and groups where the X-ray emission is undetectable. Although the search for such material is a goal of the field, at present, the sum of the galaxies and detected hot gas constitutes only about 12% of the baryons.

One of the ways of measuring the baryon content at higher redshift is through the Ly α absorbers, a technique that has been applied at lower redshift as well. A recent study at $z < 0.07$ finds that the Ly α -absorbing material accounts for $29 \pm 4\%$ of the baryon content (Penton et al. 2004; see also Sembach et al. 2004). Although this more than doubles the known baryon content, it still leaves 60% of the baryons “missing.” These baryons must be difficult to detect, and there were a variety of suggestions for the dominant state of the material. However, convergence to a prevailing model occurred rather quickly: It was argued that gas occupies low overdensity regions in the universe and has a temperature in the 10^5 – 10^7 K range. There have been many observations trying to detect this hot gas. Some measurements are secure, but others are near the detection threshold where the reality of the detections has been questioned.

In this review, we begin by examining the model predictions, where there have been significant improvements in recent years. Before reviewing the observations, many of which occur at X-ray energies, a brief review of the relevant atomic physics is given, followed by a discussion of the X-ray instrumentation and, most importantly, the limitations of such observations. This is of special importance in regard to the debates of the reality of various X-ray detections. We give a critical discussion of each of the major approaches for which the detection of the WHIM has been claimed and conclude with the expectations for the future.

2. MODELS FOR THE WARM-HOT INTERGALACTIC MEDIUM

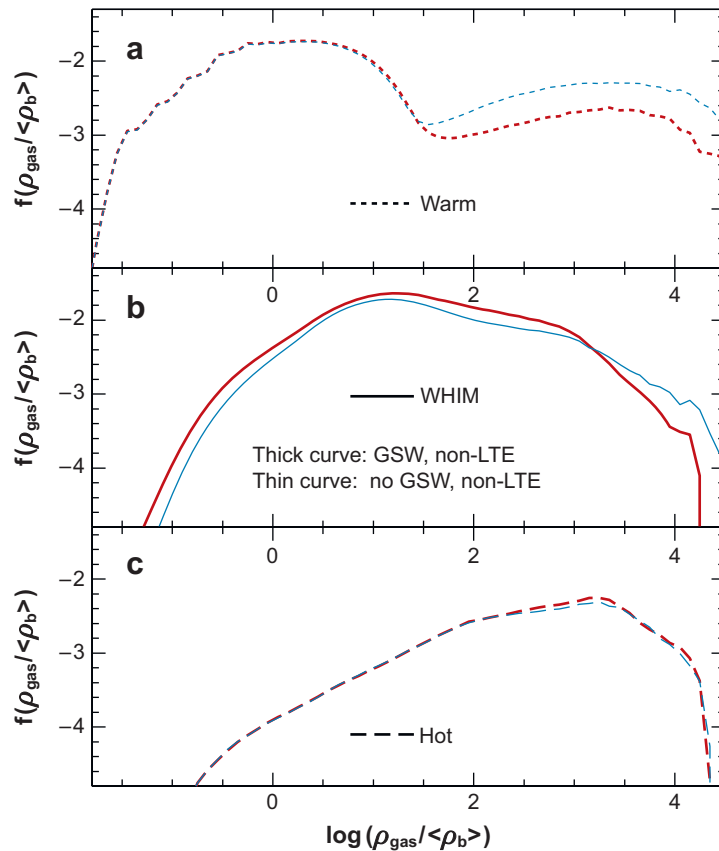
The most accurate models for the large-scale structure formation in a Λ CDM universe have been those that follow only the dark matter, as this is the dominant mass component. A gaseous component must be added to model the WHIM, along with all relevant heating and cooling processes. Following the epoch of reionization near

$z \approx 6$, most of the intergalactic medium has been photoionized to a temperature of about 10^4 K. Subsequently, the predominant heating mechanism is through the shocks that develop as large-scale density waves collapse in the dark matter (Cen & Ostriker 2006). Large-scale structure becomes more pronounced with cosmological time, so the gas is increasingly shock-heated, reaching temperatures above 10^5 K in much of the volume for $z < 1$. For overdensities of $\rho_{\text{gas}}/\langle\rho_{\text{gas}}\rangle > 160$, virialized systems such as clusters of galaxies develop with temperatures ranging from 10^7 – 10^8 K ($\langle\rho_{\text{gas}}\rangle$ is the mean cosmological density of baryons). These are easily studied by X-ray telescopes, where the current detectability limit is for $\rho_{\text{gas}}/\langle\rho_{\text{gas}}\rangle > 500$, about half of the virial radius (e.g., Pointecouteau et al. 2004).

The distribution of gas as a function of temperature and density shows that the gas ranging from 10^5 – 10^7 K generally lies in regions where the gas overdensity ranges from 10^0 – $10^{2.5}$, although with a fairly wide range, as seen in **Figure 1** (Cen & Ostriker 2006). These regions are generally collapsed but not virialized. In addition, there is hot gas in very low-density regions, the presence of which is due to shocks that propagate effectively into such environments. Such calculations, even without the effects of star formation and stellar feedback, demonstrate the fraction of gas that would be in the

Figure 1

The mass distribution of the warm gas ($T < 10^5$ K), of the warm-hot intergalactic medium (WHIM) (10^5 to 10^7 K), and of the hot gas ($T > 10^7$ K) as a function of gas overdensity in the simulation of Cen & Ostriker (2006). Most of the mass of warm gas lies at overdensities ranging from 0.03–30, whereas most of the WHIM has overdensities in the range of 1–1000, and most of the hot gas lies in the range of 30 – 10^4 .



10^5 – 10^7 K range (40% in the calculations of Cen & Ostriker 2006; see also Croft et al. 2001, Davé et al. 2001). Unfortunately, most of the observations of the WHIM involve nonprimordial elements, such as oxygen, so it is necessary to include the formation and dispersion of the heavier elements. This necessitates having a model for galaxy and star formation, for the supernova rate, for the leakage of radiation from the galaxy, and for the strength and extent of a galactic wind. There is no cosmological simulation that can calculate these physical effects from first principles, so they have to be put in by hand with educated guesses.

In their simulations with such feedback, Cen & Ostriker (2006) show that the energetics of their galactic superwinds is an order of magnitude smaller than shock heating by cosmological structures. With galactic superwinds, the predicted mass fraction of the WHIM rises from 40% to 50% at $z = 0$, although the distribution as a function of overdensity is nearly unchanged (**Figure 2**). The extent of a galactic superwind

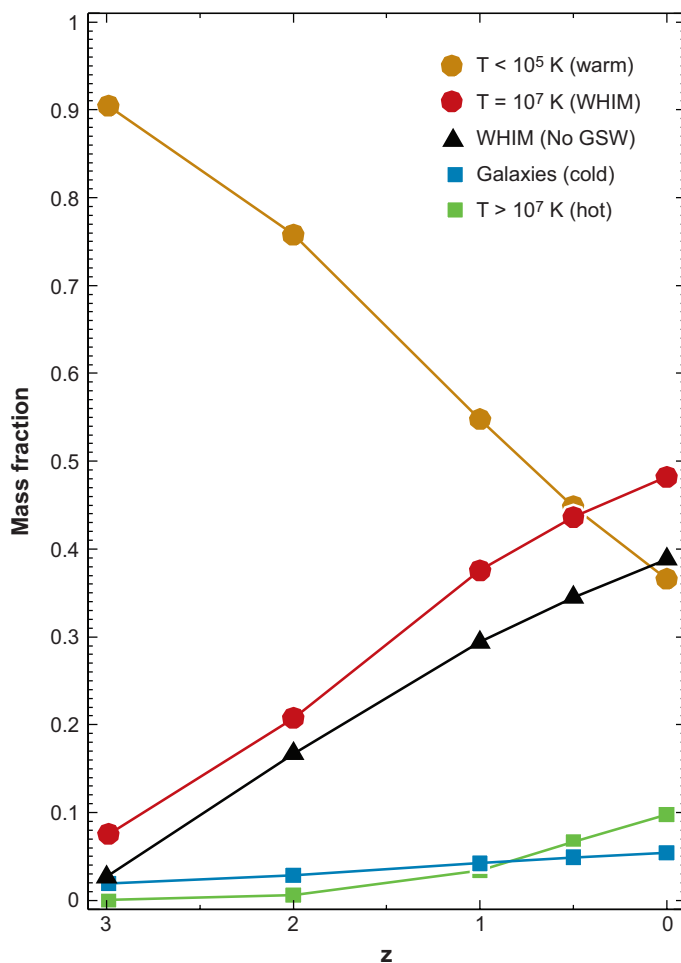


Figure 2

The evolution of the different baryonic components of the universe from $z = 3$ to $z = 0$, from the model of Cen & Ostriker (2006), where galactic superwinds (GSW) are included. The evolution of the warm-hot intergalactic medium (WHIM) component is also shown without GSWs. This is typical of other simulations that show the present-day WHIM component to be about 50% of all baryons.

establishes a lengthscale over which the metals are distributed, which was a value that had to be adopted in prior calculations. This feedback from galaxies increases the metallicity of the gas that constitutes the WHIM by about two orders of magnitude; its median metallicity is $0.18 Z_{\odot}$, with a broad range. A similar simulation, but at higher redshift (Oppenheimer & Davé 2006), finds similar results and Cen & Ostriker point out that it is difficult to constrain the galaxy wind parameters with current data.

The most common heavy element is oxygen, which has important lines for OVI, OVII, and OVIII, so the determination of the various ionic fractions is crucial. However, at the very low densities of the WHIM, the recombination times are comparable to the Hubble time for $n_{\text{H}} \approx 10^{-6} \text{ cm}^{-3}$, so nonequilibrium ionization effects need to be included, a consideration that several researchers have examined (Kang et al. 2005, Yoshikawa & Sasaki 2006, Cen & Fang 2005). There are two timescales of relevance: the recombination timescale; and the ion-electron equilibration timescale, which is usually shorter. Nonequilibrium ionization effects will extend the temperature range over which the ions are common. Because the WHIM occurs over a wide temperature range, the total predicted absorption column of an ion does not change greatly compared to collisional equilibrium ionization conditions, but the ratio of the lines from adjacent ionization states can change considerably. Therefore, the OVII/OVIII absorption line ratio will not serve as a good temperature indicator, as it does under equilibrium conditions. Emission lines are less affected by nonequilibrium effects because most readily detectable emission lines occur in relatively denser environments ($n_{\text{H}} > 10^{-5} \text{ cm}^{-3}$) where ionization equilibrium is more likely to be achieved.

There are several goals in making comparisons between the models and the data that one hopes can be achieved. The first is the identification of the missing baryons; a second is to measure their mass as a function of temperature, a central prediction (**Figure 3**). Of considerable importance is the location and topology of the WHIM. The models predict a density structure, the “cosmic web” (**Figure 4**), which is composed of the moderately high overdensity regions connecting the easily observed galaxy clusters and groups (e.g., Viel et al. 2005). Obtaining an observational description of the structure of the cosmic web, should it exist, would give us great insight into the formation of the WHIM and provide powerful constraints on the models. If structural information is available, the densities of the medium could be calculated, which would also be of significant interest. In addition, the inclusion of galactic feedback, one of the least well-constrained parts of the theory, allows for predictions for the metallicity distribution of the WHIM, so it would be valuable to confront the models with the data. As we show below, observers are struggling with the basic detection of the WHIM.

3. ATOMIC PHYSICS

In the UV region, the search for intergalactic baryons has largely focused on the detection of the OVI and HI Ly α lines. This has been widely discussed, so we only point out a few relevant items here. Hydrogen is largely ionized in the WHIM, but owing to its abundance, it may be detectable at temperatures of up to about $3 \times 10^5 \text{ K}$ if it is in collisional equilibrium (ionization fraction of 10^{-6}) and for total gas columns

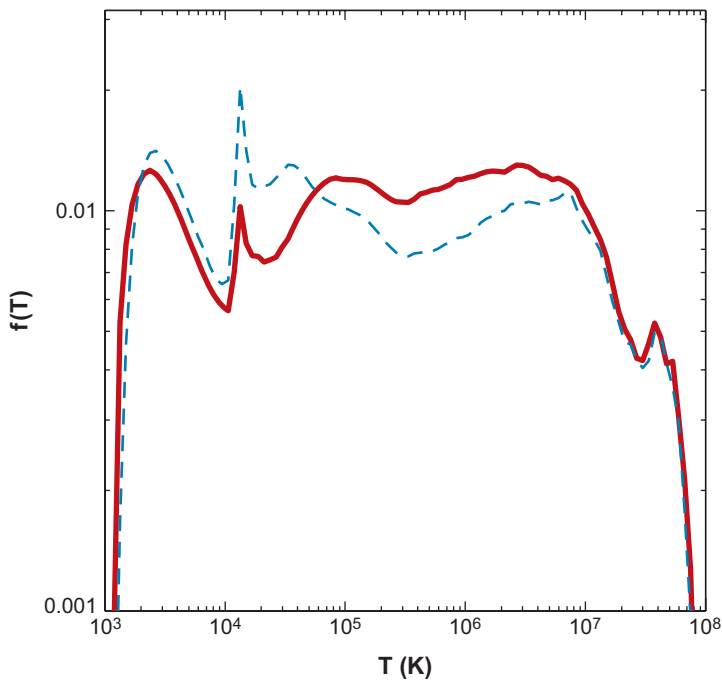


Figure 3

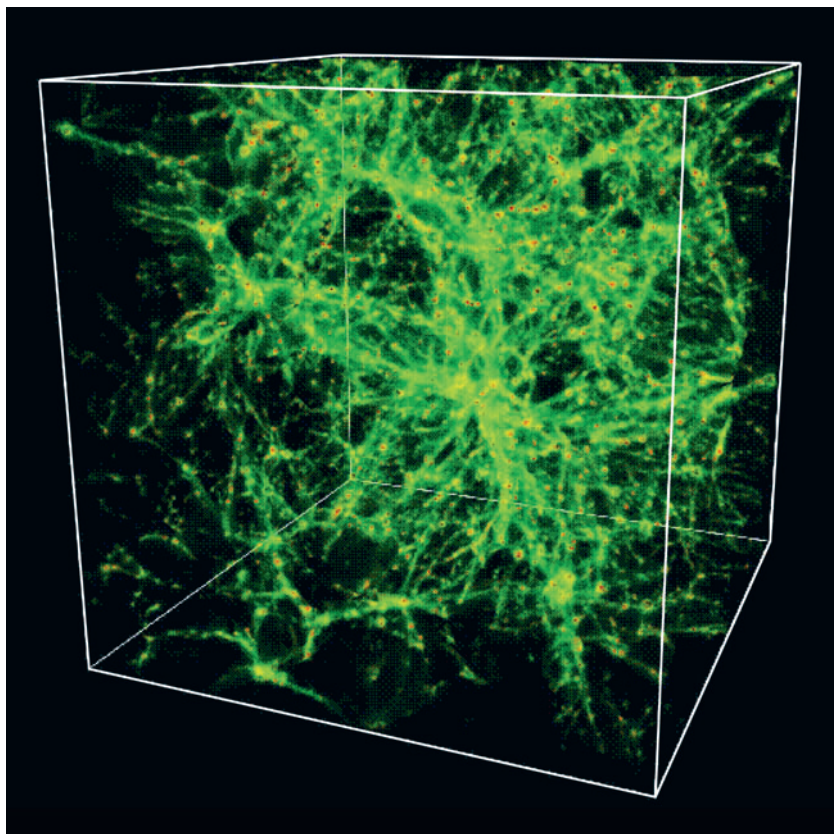
The differential mass fraction as a function of temperature for the simulations of Cen & Ostriker (2006), where the solid curve includes galactic superwinds, whereas the dashed line does not. The mass of the warm-hot intergalactic medium is fairly evenly distributed between 10^5 K and 10^7 K in the galactic superwind model. There is a local minimum in the mass fraction near 3×10^5 K, the peak temperature for the OVI absorption line diagnostic.

exceeding 10^{19} cm^{-2} (Figure 5). Unfortunately, this line will be broad (FWHM $\approx 120 \text{ km s}^{-1}$ from thermal broadening), so detecting it upon the continuum of active galactic nuclei (AGN), which are often structured, can be a challenge (discussed below). The OVI line reaches a peak fractional abundance near 3×10^5 K, and although the fractional abundance does not exceed 0.22, the cross section for the 1032 \AA , 1038 \AA ground state doublet is large. Near 3×10^5 K, this line is detectable for a total gas density $\gtrsim 10^{18} (Z/0.1 Z_{\odot}) \text{ cm}^{-2}$, making it the best probe of gas in this temperature range. Beyond 5×10^5 K, these lines are of little use and the X-ray lines become of prime importance. Owing to absorption by neutral gas in the Milky Way, there is a natural divide between the UV and X-ray regions, the former ending at 13.6 eV and the latter becoming important above 200 eV.

For gas at temperatures that emit in the X-ray band, hydrogen and helium are fully ionized, so when no metals are present, the only source of emission and absorption is by the free-free process. This process is optically thin at all X-ray energies, even when calculating the opacity over cosmological distances. The addition of metals greatly increases the emissivity of the plasma because most common species have at least one bound electron in the $0.7\text{--}10 \times 10^6$ K range. Metals contribute to the emission spectra mainly through their bound-bound lines, which are so plentiful that they form a pseudocontinuum at the typical poor resolution of X-ray imaging devices. The strongest of the lines appear distinct, with the most important ones coming from oxygen and iron. For the study of gas near 10^6 K, the strongest lines are from OVII, a helium-like species that has a ground-state triplet at 21.60 \AA

Figure 4

The density distribution for 10^5 to 10^7 K gas from a cosmological Λ CDM simulation of Cen & Ostriker (2006), where $\Omega = 0.37$, $\Omega_b = 0.049$, $\sigma_8 = 0.80$, and where $L = 100 \text{ h}^{-1} \text{ Mpc}$. Most of the mass of the warm-hot intergalactic medium lies within the filaments that connect the higher density region.



(a permitted line; $1s-2p$; 574 eV), 21.80 \AA (semiforbidden), and 22.10 \AA (forbidden). Although only the resonance line is important for absorption, the other lines can be more important in emission observations. Another important species (at higher temperature) is hydrogenic oxygen (OVIII), for which the equivalent of the $\text{Ly}\alpha$ line occurs at 18.97 \AA (654 eV). Other absorption lines of note are NVII $\lambda 24.78$, NeIX $\lambda 13.45$, and the $\text{Ly}\beta$ line of OVII at 18.63 \AA (this is a highly incomplete list), whereas FeXVII and related ions are responsible for a variety of lines that are more useful in emission observations.

Even though the product of the peak ionization fraction and the oscillator strength is higher for OVII than for OVI, the column needed to achieve a detectable equivalent width is significantly larger for OVII. This is because the fractional equivalent width of a transparent line is inversely proportional to the energy of the transition, and as the transition energy for the OVII $\lambda 21.60 \text{ \AA}$ line is a factor of 50 greater than that of the OVI $\lambda 1032 \text{ \AA}$ line, the fractional equivalent width is significantly smaller. Furthermore, optical instruments have an advantage in that they resolve the OVI $\lambda 1032 \text{ \AA}$ line, whereas the OVII $\lambda 21.60 \text{ \AA}$ line is not resolved by current X-ray instruments, typically by a factor of 2–6 (the signal-to-noise is proportional to

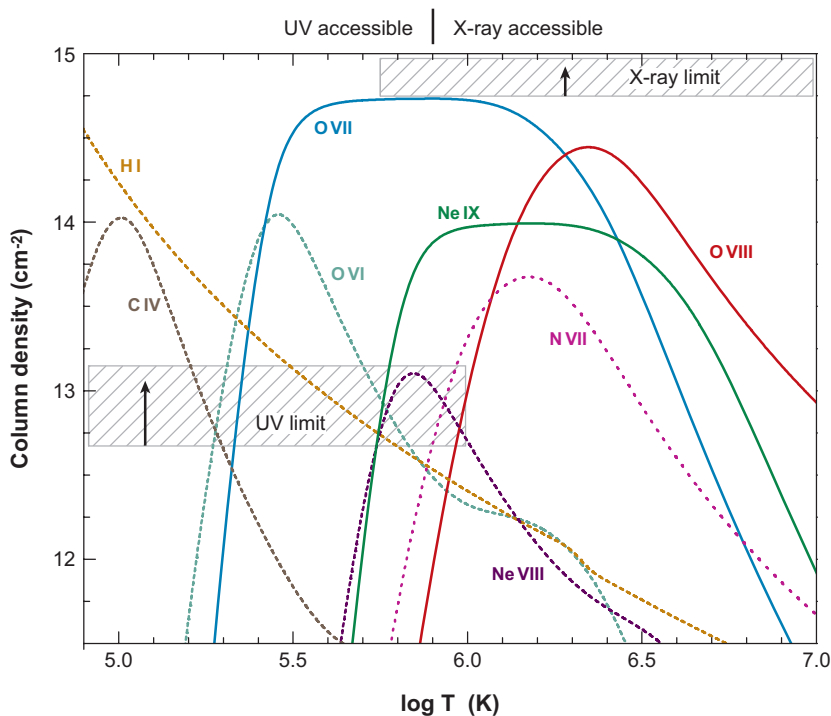


Figure 5

The ion fraction distributions, represented as column densities for a total gas column of 10^{19} cm^{-2} and metallicities of $0.1 Z_{\odot}$. The UV lines are effective at detecting absorbing gas for $T < 5 \times 10^5 \text{ K}$ and currently have significantly better sensitivity than the X-ray OVII $K\alpha$ and OVIII $K\alpha$ lines, which are good diagnostics for gas temperatures ranging from 0.5 to $5 \times 10^6 \text{ K}$. Absorption by OVII, OVIII, and NeIX have been detected at $z = 0$, probably because of the higher metallicity of Galactic Halo gas. The NVII ion (*dotted*), which has a hyperfine line in the radio region, is also shown.

the resolving power for an unresolved line). At 0.1 of the solar metallicity and for a temperature of 10^6 K , the column needed for a detection toward a strong X-ray source is $1\text{--}10 \times 10^{19} \text{ cm}^{-2}$. The width of the line is $\text{FWHM} = 54 (T/10^6)^{1/2} \text{ km s}^{-1}$ if it is at the Doppler width for oxygen, but the sound speed in the gas is $150 (T/10^6)^{1/2} \text{ km s}^{-1}$, so if there is sonic turbulence, the FWHM could be closer to 200 km s^{-1} . Also, large-scale motion in filaments can easily produce velocity widths of a few hundred km s^{-1} . These line widths imply that the resolutions needed to resolve the lines are $E/(\Delta E) = 1000$ to 3000 . However detections can be obtained with a resolution of only a few hundred (the resolution for *Chandra* and the *X-ray Multi-Mirror Mission-Newton (XMM-Newton)* near the OVII line is about 400).

4. X-RAY INSTRUMENTATION

Unlike optical and UV detectors, where one integrates over time and collects many photons before readout, X-ray solid-state detectors count single photons. This is possible because of the relatively slower count rate but there is an enormous advantage to the technique in that the number of holes created in the CCD is proportional to the X-ray photon energy. Therefore, the energy of the input photon is determined to $50\text{--}200 \text{ eV}$, leading to a resolution of $10\text{--}60$, depending on the detector and the energy region ($0.5\text{--}10 \text{ keV}$). This yields a low-resolution spectrum at every location and permits many narrow-band images to be constructed. When the incoming signal

is dispersed through reflection or transmission gratings, higher resolution is reached, although with a loss of an order of magnitude or more in throughput. At energies below 1 keV, resolutions of 400–1200 are achieved with *XMM-Newton* and *Chandra* (Jansen et al. 2001; Weisskopf 2003), which is sufficient to begin resolving the lines.

The sensitivity of these X-ray detectors is not uniform over their energy band and the calibration of the detectors can change in unpredictable ways after launch. At energies below 1 keV, there is usually a significant low-sensitivity region from 0.28 keV to about 0.4 keV owing to photoelectric absorption from carbon in the optical path. At energies below about 0.3 keV, the *Chandra* backside illuminated CCDs have no sensitivity, while the *XMM-Newton* EPIC (European Photon Imaging Camera) can detect photons to below 0.2 keV, but with lower sensitivity. The changes in sensitivity (the calibration) often are monotonic in energy with the lower energies being most greatly affected. This is probably due to outgassing and subsequent deposition onto the surfaces of the mirror, gratings, or entrance window. Recalibration of the instrument in flight is a difficult process because there is no ideal celestial calibration source, but through clever approaches, moderately good recalibration has been accomplished. Improper calibration can lead to mistakes in determining the presence of weak emission features, such as from the WHIM.

Another serious issue is the flat-fielding of the data, which must be properly accomplished if one is to measure faint extended emission structures. The fields of view are typically from 8 to 30 arcmin, depending on the instrument used. The outer parts of these fields are vignetted because the nested mirror design leads to one mirror shell shadowing another. This vignetting function can be measured accurately for photons coming down the optical axis, but there is a background component that is not focused and it can change with time. In addition, there are several focused backgrounds: one due to plasma processes in the Solar System; one due to diffuse gas in the Local Bubble and above the disk of the Galaxy; and one due to AGNs. The first one varies in time and can produce dramatic background flares. The second varies around the Galaxy, and although it is roughly known (Snowden et al. 1997), it is not known with precision on the scale of *Chandra* or *XMM-Newton* fields. Separating these components so that one truly has a flattened image of the field at energies below 1 keV is challenging and can be the limiting step in identifying diffuse structures.

5. DETECTION OF THE $1\text{--}5 \times 10^5$ K WARM-HOT INTERGALACTIC MEDIUM

At UV wavelengths, the fractional equivalent width of absorption lines is a factor of 30 larger than at X-ray energies (for the same oscillator strengths). Thus, the resolution of detectors is often sufficient to resolve the lines [e.g., *Far Ultraviolet Spectroscopic Explorer* (FUSE), and a telescope such as the *Hubble* (HST), has considerably more collecting area than *XMM-Newton* or *Chandra*]. These are substantial advantages, and there are two strong lines that can be used to trace the WHIM at temperatures below 10^6 K, OVI, and the hydrogen Ly α line. Under collisional ionization conditions, the lithium-like species OVI never becomes the dominant ion, having a peak ionization

fraction of about 0.25. Furthermore, it is present in only a narrow temperature range (an ionization fraction above 0.025 for $2\text{--}5 \times 10^5$ K), whereas OVII has a significant ionization fraction over nearly an order of magnitude in temperature. However, with the ability to detect OVI columns down to 10^{13} cm⁻², compared to typical X-ray limits of nearly 10^{15} cm⁻², and the prediction that there are significant amounts of the WHIM at $\sim 10^{5.5}$ K, the UV should be a better hunting ground for detecting the WHIM, and studies have borne out this expectation.

Although OVI had been observed in absorption toward higher redshift systems, the first low redshift detection was obtained by Tripp et al. (2000), with a half-dozen systems reported by Savage et al. (2002). There have been subsequent studies, and a large statistical sample to date is presented in Danforth & Shull (2005), who used FUSE and searched for OVI in 129 known low redshift Ly α absorption line systems ($z < 0.15$) in sightlines toward 31 AGN. They detected OVI absorption in 40 systems with column densities of $\log N(\text{OVI}) = 13.0$ to 14.5 and they derive the equivalent width distribution to show that the lower column density systems contribute about the same baryonic mass as at higher column densities. They determine the space density of OVI (to a limit of 30 mÅ) of $dN(\text{OVI})/dz \approx 17$ (20% uncertainty), from which they determine the contribution to the WHIM of $\Omega_{\text{WHIM}} = 0.0022 \pm 0.003 (Z_{\text{O}}/0.1Z_{\odot})^{-1} (f_{\text{OVI}}/0.2)^{-1}$, or about 5% of the baryon content. This is a lower limit to the WHIM from $10^{5.5}$ K gas because undetected lower column density absorption lines could contribute significantly.

A slightly larger and somewhat different sample was compiled by Tripp et al. (2006) by using STIS (Space Telescope Imaging Spectrograph) on HST to observe 16 AGNs where they find 44 intervening OVI absorbers. As the OVI line was redshifted into the STIS bandpass, the redshift of the absorbers ($0.12 < z < 0.57$) is larger than the sample of Danforth & Shull (2005). Tripp et al. (2006) find a slightly larger OVI absorption frequency, $dN(\text{OVI})/dz = 23 \pm 4$ for absorption lines with equivalent widths greater than 30 mÅ. Their measured OVI contribution to the baryon fraction is correspondingly greater at 7%. The fraction of WHIM material is predicted to decrease with decreasing redshift, so the absorption frequency determined from the STIS data might be expected to be 20–30% lower than the data set obtained with FUSE, whereas the opposite is observed. If the model predictions are correct, then the absorption frequency $dN(\text{OVI})/dz$ differs at the 2σ level between the two data sets. It is important to resolve this possible discrepancy and also to extend the surveys to lower equivalent widths, as Danforth & Shull (2005) find that these may add a significant contribution to the mass fraction of gas in this temperature range.

The size of these OVI absorption line samples permits investigators to determine whether the material is associated with galaxies. Early studies suggested that the OVI lay within a few hundred kiloparsecs of a galaxy, but for this statement to be made more quantitatively, the chance coincidence with random galaxies must be accounted for. Stocke et al. (2006) used the FUSE sample along with several galaxy catalogs, and they found that for galaxies of luminosity L_* or brighter, their median separation was 1.8 Mpc, but the distance from a OVI absorber to a galaxy was only 0.6 Mpc. Nearly all of the OVI absorbers are found at distances of < 0.8 Mpc of a galaxy with $L \geq L_*$ and this gives a maximum characteristic sphere of influence around the galaxy

for the deposition of the metal-rich WHIM near $10^{5.5}$ K. This is a maximum size scale because smaller galaxies can enrich the intergalactic medium. When galaxies with $L \leq 0.1L_*$ are considered, the distance from an OVI absorber to a galaxy falls to 0.34 Mpc. Stocke et al. (2006) argue that to reproduce the observed $dN(\text{OVI})/dz$, yet fainter galaxies must contribute to the absorption. The sphere of influence of galaxies is consistent with that predicted from models.

Another approach to detecting the WHIM at lower temperatures is through neutral hydrogen. Because of its much larger abundance, although its ionization fraction is decreasing rapidly near 10^5 K, it has a larger column density than OVI for $T < 2 \times 10^5$ K (for $Z_{\text{OVI}} = 0.1Z_{\odot}$). An advantage to using hydrogen is that this is the primary mass component, but the disadvantage is that the ionization correction is quite large and the determination of the temperature is uncertain. The temperature could be determined from the line width measurement if thermal broadening were the only broadening mechanism, and there are lines observed that are sufficiently broad to have temperatures above 10^5 K (Richter et al. 2004; Sembach et al. 2004); $T = 1 \times 10^5 (b/40 \text{ km s}^{-1})^2$ K, where b is the usual line width parameter ($\text{FWHM} = 1.665b$). The largest survey is that of Lehner and colleagues (N. Lehner, B.D. Savage, P. Richter, K.R. Sembach, T.M. Tripp, & B.P. Wakker, submitted), who estimate that approximately 20% of the local baryons may be associated with highly ionized hydrogen. The primary difficulty with this method is that the line width can be broadened by bulk or turbulent motions in a much cooler gas. Also, multiple unresolved 10^4 K absorption components can blend together to mimic a broader line from an apparently hotter medium. Lehner and colleagues address these problems through simulations, and while these may resolve such issues, we note that it is notoriously difficult for models to properly reproduce turbulence, which can be responsible for the broad lines. If the identification of intrinsically broad lines can be shown to be truly reliable, the HI Ly α absorption would be a valuable tool in measuring the WHIM near 10^5 K.

Finally, an ionization line with a characteristic temperature greater than OVI has been detected in the UV region, NeVIII, although only at the 3.9σ level (Savage et al. 2005). The NeVIII ion is lithium-like and never even achieves a maximum ion fraction in excess of 15%, which occurs near 7×10^5 K, about twice the temperature at which OVI has its maximum ionization fraction. Because the ionization fraction distribution for lithium-like species is narrow, there is only a very limited temperature range when both OVI and NeVIII may be present (at $\log T = 5.70$, $f_{\text{NeVIII}} = 0.021$ and $f_{\text{OVI}} = 0.026$ in collisional ionization equilibrium). So while it is possible to produce both lines in the same gas, as Savage et al. (2005) suggest, the lines are equally likely to occur from different temperature regions where the ionization fractions are an order of magnitude higher. The total column density that Savage et al. (2005) suggest would account for a NeVIII detection is nearly 10^{20} cm^{-2} , which would be an unusually high column density filament (from theoretical modeling), large enough to produce detectable X-ray absorption lines in OVII. This NeVIII λ 770.4 line requires a redshift of 0.3–0.5 to appear in the FUSE band and $z > 0.53$ to lie in the HST band, so if it can be detected at high significance and in other sightlines, it will be a useful indicator of the WHIM at intermediate redshifts.

6. THE WARM-HOT INTERGALACTIC MEDIUM CONTENT IN THE LOCAL GROUP

The mass of hot gas in galaxy groups is not well determined because at the last radius where X-ray surface brightness is usually measured, the gas mass is rising as r^m , where $m \approx 1.5$ (e.g., Mulchaey 2000). Therefore, it is possible that galaxy groups may possess a cosmologically significant baryon content, and because the Milky Way lies in a typical galaxy group, it offers an ideal opportunity for study, both through emission and absorption.

X-Ray absorption line studies are practical for the brightest AGNs and the first identification of absorption line gas at $z \approx 0$ was reported by Nicastro et al. (2002) for *Chandra* observations of PKS 2155-304, shortly followed by Rasmussen et al. (2003), who reported on *XMM-Newton* observations of 3C 273, Mrk 421, and PKS 2155-304. Both groups agree that the OVII K α (21.60 Å) and the OVIII K α (18.97 Å) lines are detected in PKS 2155-304, although Nicastro et al. (2002) report the detection of a NeIX K α (13.45 Å) while Rasmussen et al. (2003) report an upper limit. For the OVII and OVIII lines in PKS 2155-304, both groups agree that the ion columns are about $5 \times 10^{15} \text{ cm}^{-2}$ in the low opacity limit, so the difficulty is how one converts this into a mass of gas. The conversion requires values for the ionic fractions and a path length, and it is the choice of the path length that can give rise to vastly different values for the inferred gaseous mass.

The first analysis of the X-ray absorption by Nicastro et al. (2002) led them to conclude that the hot gas fills the Local Group and has a mass of $\sim 10^{12} M_{\odot}$, significantly more mass than the sum of the galaxies. However, this result is model-dependent. They assume that the X-ray absorption lines from OVII and OVIII, as well as the UV absorption lines from OVI, originate in the same gas (along with NeIX). In the X rays, the lines are unresolved and the velocity uncertainty is about 250 km s^{-1} for the OVII K α line and 450 km s^{-1} for the OVIII K α line. At UV wavelengths, the FUSE measurements reveal two components at 36 km s^{-1} and -135 km s^{-1} ($\pm 10 \text{ km s}^{-1}$), so from the current information, it cannot be shown that any of the lines are at the same velocity. Nicastro et al. consider single-temperatures models of a gas at a variety of densities and they include photoionization effects from the X-ray background. They can accommodate the observed lines in a low density plasma (10^{-6} cm^{-3}), but the path length is 15 Mpc ($0.3 Z_{\odot}$ abundances). However, this is excluded because a path length of this magnitude would show the effects of Hubble expansion, shifting the lines in velocity space. To obtain an acceptable solution, they assume that only the weaker and broader OVI line (25% of the total column) is associated with the X-ray absorbing gas, leading to a solution for $n_e = 6 \times 10^{-6} \text{ cm}^{-3}$, Ne/O = 2, and a path length of 3 ($0.3/[\text{O}/\text{H}]$) Mpc. This is larger than the virial radius for a group of galaxies (1 Mpc), and their path length would become 10 Mpc for $[\text{O}/\text{H}] = 0.1$, which may be more representative of the WHIM. They admit the possibility that there could be a multitemperature gas, and that would modify their results significantly.

A different approach was taken by Rasmussen et al. (2003), who assume that the OVII K α and OVIII K α lines are cospatial but that the OVI λ 1035 doublet is from a

spatially different region. Unlike Nicastro et al. (2002), they do not detect the NeIX $K\alpha$ in PKS 2155-304 (which had produced a larger NeIX column than either the OVII or OVIII column), but they detect it in Mrk 421, with a column ($1.5 \times 10^{15} \text{ cm}^{-2}$) that is half to one-third of the oxygen columns ($4.8 \times 10^{15} \text{ cm}^{-2}$ for OVII and $2.4 \times 10^{15} \text{ cm}^{-2}$ for OVIII). This reduction in the column ratio of Ne/O also reduces the elemental ratio to near-Solar values. The observed OVIII/OVII line ratio is used to set the temperature in a collisional ionization equilibrium model. They establish a maximum lengthscale of 2 Mpc by requiring that Hubble flow does not shift the line center beyond its observed value (when errors are included). This implies that $n_e > 5 \times 10^{-5} \text{ cm}^{-3}$ and, at such densities, the ambient X-ray background should not significantly modify the ionization distribution. They argue for a minimum length scale of 140 kpc by requiring that the soft diffuse emission not be exceeded. They favor a size for the absorbing region in the 100–1000 kpc range, which would make this more of a Local Group medium than a Galactic halo medium, with a mass of 10^9 – $10^{11} M_\odot$.

Although both approaches require that their models not exceed the observed diffuse X-ray background emission, they do not make use of the emission, for which a single high-resolution spectrum was obtained with a quantum microcalorimeter toward $l, b = 90^\circ, 60^\circ$ and with a 1 sr field of view (McCammon et al. 2002). This spectrum showed that the strongest single feature was the OVII $K\alpha$ triplet and this yields an emission measure for OVII, given a temperature and metallicity. When combining the absorption and emission measures for OVII and for an ion fraction of 50%, the lengthscale becomes about 20 kpc, with $n_e = 9 \times 10^{-4} \text{ cm}^{-3}$, or a gas mass of $4 \times 10^8 M_\odot$ (Sanders et al. 2002; Bregman & Lloyd-Davies 2007). A similar result is obtained by using the emission measure inferred from the *Rosat* broad-band data of Snowden et al. (2000), as shown by Fang et al. (2006). In this analysis, the gas is in a Galactic halo and the gas mass is an order of magnitude less than the neutral gas content of the Galaxy. This gas most likely came from the disk and was heated by supernovae, so the assumption of Solar abundance for the metallicities is justified. For this model to be correct, some if not most of the OVIII absorption comes from a slightly hotter gas (0.1–0.2 dex), but most realistic systems have temperature fluctuations. Also, if the filling factor were less than unity, the halo would be larger. A minimum size to the halo can be derived by assuming an ionization fraction of unity for the OVII, which leads to a lengthscale of 5 kpc.

Subsequent studies have sought to clarify which models are most likely. The largest lengthscale model advocated by Nicastro et al. (2002) is unlikely to be valid, based on several studies. Williams et al. (2005) show that, for a sightline toward Mrk 421, the OVI λ 1032 absorption line has a larger Doppler parameter than for the OVII λ 21.60 line. They further argue that this Doppler parameter is inconsistent with the OVI (HVC)/OVII ratio (they make similar arguments for an observation toward Mrk 279; Williams et al. 2006). For the same sightline toward Mrk 421, Savage et al. (2005) show that the OVI absorption between -140 km s^{-1} and 60 km s^{-1} is associated with low-ionization gas in the Galactic thick disk/halo. For the higher velocity gas, from 60 – 165 km s^{-1} , absorption by CIII is also seen, and based on the column density ratio $N(\text{OVI})/N(\text{CIII})$, they argue that this gas cannot coexist with OVII and OVIII at the same temperature.

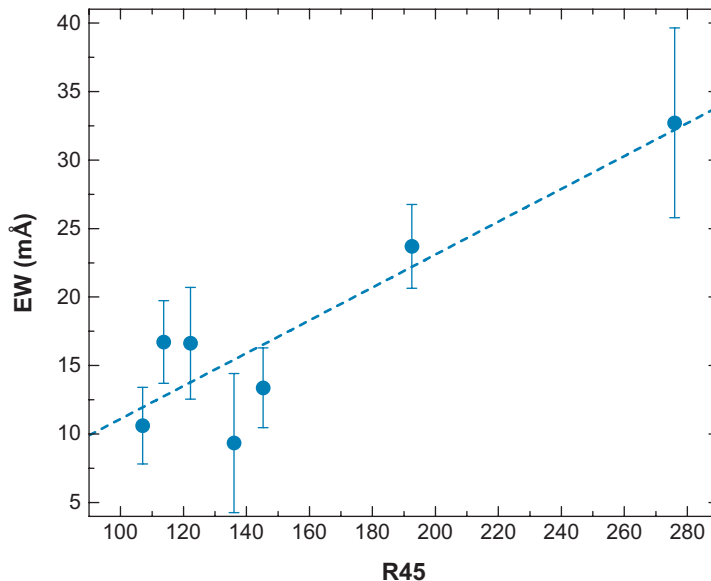
Some researchers argue that the OVII and OVIII absorbing gas is produced in a Galactic halo rather than a Local Group medium. They analyze a set of $z \approx 0$ absorption lines detected toward a sample of the brightest AGNs using both *Chandra* and *XMM-Newton* observations (Wang et al. 2005; Fang et al. 2006; Bregman & Lloyd-Davies 2007). One of the distinguishing properties is whether the absorbing gas has a redshift similar to the Milky Way (0 km s^{-1}) or to the Local Group (-250 km s^{-1}). This difference is less than the instrumental resolution (HWHM $\approx 400 \text{ km s}^{-1}$), but a line center can be determined more accurately than the instrumental resolution. For a *Chandra* observation toward LMC X-3, Wang et al. (2005) find an absorption line velocity of 56 km s^{-1} ($-83, +194 \text{ km s}^{-1}$), which is more suggestive of a Galactic halo origin. Bregman & Lloyd-Davies (2007) used the data from the four highest signal-to-noise absorption line systems (observations with *XMM-Newton*), where the random uncertainty in the calibration of a single observation is 111 km s^{-1} . They find a mean velocity of $70 \pm 55 \text{ km s}^{-1}$, which is consistent with the Milky Way velocity but 4.6σ different from the Local Group velocity. The absorption lines studied by others are consistent with a velocity near 0 km s^{-1} and an origin from Galactic halo gas (e.g., Rasmussen et al. 2006).

Another argument is given by Fang et al. (2006) who show that if the absorption lengthscale were 1 Mpc, and if this were typical of galaxy groups, intergalactic absorption would easily and commonly be detected as the sightlines of AGNs pass through relatively common galaxy groups. Their constraint indicates that the lengthscale be less than about 0.5 Mpc (at the 99% confidence limit), and this might be improved by making this test with the higher S/N *XMM* data.

Additional insight may be gained by determining whether the distribution of absorption line strengths has a Galactic dependence or a Local Group dependence. If there were a halo around the Galaxy with a radius of $\lesssim 30 \text{ kpc}$, lines of sight across the Galaxy would have greater absorption than those away from the Galaxy. The Local Group has a different signature caused by its elongation toward the MW-M31 axis, with the largest column toward M31 and the smallest column in the anti-M31 direction. By good fortune, the anti-M31 direction is toward the bulge of the Milky Way ($l, b = 301^\circ, 22^\circ$), where the Galactic halo model predicts the greatest absorption columns. This makes the two models nearly orthogonal, which is the ideal situation. To define the angular distribution of columns, Bregman & Lloyd-Davies (2007) used a sample of 26 extragalactic lines of sight, 17 of which have uncertainties in the OVII $K\alpha$ equivalent width of 10 m\AA or less (the median equivalent width is about 20 m\AA). The data show no enhancement in the sightlines within 30° of M31, nor is there a minimum in the equivalent widths toward the anti-M31 direction. However, there is a correlation between the equivalent widths and the Galactic $3/4 \text{ keV}$ background, which measures the emission from gas in and around the disk, including a halo (**Figure 6**). This adds to the evidence that the OVII gas is primarily of Galactic origin, probably of radius 10–50 kpc. A hot halo of similar size is seen in the recent *Chandra* X-ray observation of the massive spiral NGC 5746, where X-ray emission extends to at least 20 kpc (Rasmussen et al. 2006). The estimated gas mass is $3 \times 10^9 M_\odot$ for a metallicity of $0.04 Z_\odot$. This metallicity is uncertain and, as the derived mass varies approximately inversely with the square root of the metallicity,

Figure 6

The OVII equivalent width as a function of the Galactic R45 intensity (3/4 keV) where the 26 sample objects have been binned into seven groups (Bregman & Lloyd-Davies 2007). The correlation of the two quantities suggests that most of the OVII absorption has a Galactic origin, probably caused by a halo of size 15–100 kpc.



the mass would be several times smaller for a metallicity of $0.3 Z_{\odot}$. This mass estimate is a few times larger than that inferred for the extended halo around the Milky Way.

A final consideration that bears upon this is observations involving the Magellanic Stream, cold gas that has been torn from the LMC/SMC system by the gravitational tidal forces of the Milky Way (Mastropietro et al. 2005, Connors et al. 2006). There are indications that the Magellanic Stream is interacting with a dilute medium, both from ionization and structural considerations. The Stream is composed of a variety of clouds and the surfaces of the clouds in the predicted direction of motion (along the Stream toward the LMC/SMC) are bright in $H\alpha$. This led Weiner & Williams (1996) to argue that the emission was shock heated owing to an interaction with a gas where $n \gtrsim 10^{-4} \text{ cm}^{-3}$ (more recently and thoroughly discussed by Putman et al. 2003). If the Stream clouds are pressure confined by the hot medium, $n \lesssim 3 \times 10^{-4} \text{ cm}^{-3}$ (Stanimirović et al. 2002). Lower estimates of the density are given by Sembach et al. (2003), who argue that some of the OVI absorption detected by FUSE occurs at the boundaries between clouds ($T \lesssim 10^4 \text{ K}$) and the 10^6 K medium (with $n \lesssim 10^{-4} - 10^{-5} \text{ cm}^{-3}$). Also, Murali (2000) suggests a density $< 10^{-5} \text{ cm}^{-3}$ if the clouds are to survive evaporation by thermal conduction, but as Mastropietro et al. (2005) point out, the density limit may be an order of magnitude higher for a lower (but sensible) choice of temperature. Also, in their gravitational and hydrodynamic modeling of the Stream, Mastropietro et al. (2005) argue that a model with hot dilute gas improves the results, where they choose a mean density of $8.5 \times 10^{-5} \text{ cm}^{-3}$ within 50 kpc. A total hot gas density of 10^{-4} cm^{-3} would lead to an electron column density of $1 \times 10^{-19} \text{ cm}^{-2}$, which would only contribute 20% to the mean inferred OVII $K\alpha$ equivalent width for Solar abundance (and a mass of $6 \times 10^8 M_{\odot}$).

At greater radii, there is a useful density estimate from Blitz & Robishaw (2000) who point out that the nearer dwarf galaxies are devoid of cold gas while the more distant ones sometimes have HI. They attribute this difference to ram pressure stripping and derive a value for the gas density of $2.5 \times 10^{-5} \text{ cm}^{-3}$ at a distance of 200 kpc. This also corresponds to an electron column density of $1 \times 10^{-19} \text{ cm}^{-2}$, so it would never dominate the OVII K α equivalent width, although the gas mass would be $1 \times 10^{10} M_{\odot}$. This gas mass is about 15% of the baryonic content within 200 kpc, so it is an important but not dominant component.

To summarize, these studies indicate that the Milky Way has a hot gaseous halo that produces the observed OVII K α absorption and the gas has a temperature near 10^6 K and a mass of $4 \times 10^8 (l/20 \text{ kpc})^2 M_{\odot}$. A more dilute gaseous medium probably extends through the Local Group and with a mass of $\sim 10^{10} M_{\odot}$, which provides only a modest contribution to the total baryon content. There are fewer constraints on the gas containing OVIII, as its absorption line is less commonly detected. It may arise in the Local Group medium or in the hotter regions surrounding the Galaxy, if there are regions where the gas temperature is near $10^{6.3} \text{ K}$.

7. X-RAY ABSORPTION DETECTION BY THE WARM-HOT INTERGALACTIC MEDIUM?

The detection of the WHIM in the X-ray lines would reveal gas at 10^6 – 10^7 K and open a new line of research that is complementary to the detection of cooler gas through the UV lines. This is a pioneering area that has been the focus of much attention and observing time, which is justified by the magnitude of the issue involved. Our belief is that the evidence for a discovery of this importance must be compelling and, by this criterion, it is unlikely that there has been a detection of dilute 10^6 – 10^7 K gas beyond the Local Group.

The primary claim for the detection of the 10^6 – 10^7 K WHIM comes from the observation of Mrk 421, the brightest AGN at X-ray wavelengths, and because this is a featureless BL Lac object, it is an ideal target against which to search for absorption lines. As discussed above, the strongest line is expected to be the 21.6 Å resonance line of OVII, although other lines, such as the 18.97 Å Ly α line of OVIII, could be strong for temperatures near 10^6 – 10^7 K .

Nicastro et al. (2005) reported on two long (96–100 ksec) *Chandra* observations of Mrk 421, one taken with the LETG (Low-Energy Transmission Grating) in combination with the High Resolution Camera (HRC) and one with the LETG in combination with the ACIS (AXAF CCD Imaging Spectrometer) CCD array. These observations were obtained when Mrk 421 was particularly bright, so they obtained 2.7×10^6 photons (HRC) and 4.3×10^6 photons (ACIS; Kaastra et al. 2006), or a combined amount of about 5500 photons per 50 mÅ bin near 21.6 Å. They combined the data from the two instruments for their analysis. Ideally, one would like to fit a simple spectral model, such as a power law with Galactic absorption, and then identify spectral features in the normalized spectrum. When Nicastro et al. (2005) tried this, enormous residuals resulted. They show that these residuals are due to calibration errors near elemental absorption edges. To deal with this calibration problem, they

fit a power law plus absorption, but the abundances of the absorbing gas were permitted to have values significantly different from those of Galactic interstellar gas. This procedure is meant to account for contaminating material in the optical path of the instrument in addition to the usual absorption by Galactic interstellar gas. A much better fit was obtained with C and Ne abundances about three times the Solar value while N and O were nearly absent. Following this procedure, there were still a number of significant deviations in their spectral fit, so they added 10 broad Gaussian features, six in emission and four in absorption. This fitting procedure, which includes unphysical abundances and arbitrary Gaussian components, is used to produce a flattened spectrum. From this flattened spectrum, they begin a search for physically meaningful absorption lines.

This flattened spectrum requires that additional line components be added, because the quality of the fit was unacceptable, having a χ^2 of 2892 for 1598 degrees of freedom. They point out that the largest remaining deviations were clearly identified with absorption at $z = 0$. Consequently, they added 24 absorption line fits and this reduced the χ^2 to 1911 for 1529 degrees of freedom; this is the final normalized data set. Although this is a significant reduction in χ^2 it still is not an acceptable fit, with a probability of occurrence much smaller than 10^{-4} .

They examine whether any of the 24 absorption lines lie at redshifts between Mrk 421 ($z = 0.030$) and $z = 0$, and they find two weak absorption line systems at redshifts of 0.011 and 0.027. The strongest line is the OVII 21.60 Å line at $z = 0.011$, for which they find a significance of 3.8σ . This significance results from a Gaussian fit where all Gaussian parameters and the continuum are free to vary. There are no other lines at this redshift above the 3σ level, but they identify two nitrogen lines (NVI K α and NVII K α) at the 3.0σ and 3.1σ level and the OVII 21.60 Å line (2.8σ) with a redshift of 0.027. An equally strong absorption line at 24.97 Å has no identification. The OVI λ 1032 line is not detected at these redshifts with FUSE. This is an important nonconfirmation because the OVI line should exist at about the same temperature as the NVI line and FUSE is sensitive to columns two orders of magnitude smaller than this *Chandra* observation. A HI Ly α line is detected at $z = 0.01016$, but the column is orders of magnitude smaller than that needed to produce the X-ray N or O lines. This is not necessarily a conflict as the ionization temperatures of these species are quite different. Based on the column density and frequency of the X-ray lines, Nicastro et al. (2005) calculate a cosmological mass density for the WHIM that would be consistent with model predictions. If this is correct, it constitutes the discovery of the hot missing baryons.

The detection of these lines has been questioned (Kaastra et al. 2006, Rasmussen et al. 2006), mainly using *XMM-Newton* data but also using 244 ksec of *Chandra* calibration data for Mkn 421 taken about a year after those by Nicastro et al. (2005). The sum of the calibration data provide a spectrum of 3.2 million photons, about 20% more than the LETG/HRC spectrum and 25% fewer photons than the LETG/ACIS spectrum reported by Nicastro et al. (2005). Kaastra et al. (2006) reanalyze the *Chandra* data, including these calibration observations and an additional LETG/HRC observation from 2000. Instead of fitting a spectral model, they fit a 12-point spline with nodes separated by 0.5 Å, and they removed the strongest instrumental features

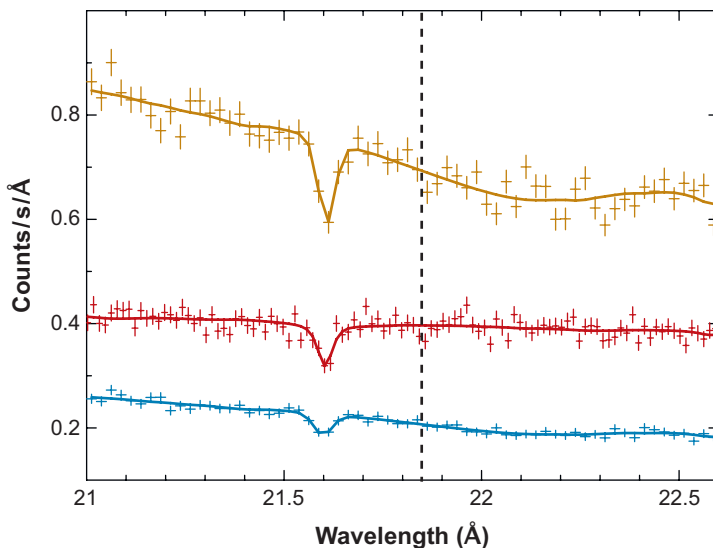


Figure 7

The 21.0–21.6 Å spectrum of Mrk 421 obtained with the *Chandra* Observatory and reduced by Kaastra et al. (2006). The top spectrum is the LETG/ACIS observation when Mrk 421 was brightest, the middle spectrum is the sum of the LETG/HRC-S observations and the bottom spectrum is the more recent calibration observations taken with the LETG/ACIS (it is brighter than the middle spectrum but has been displaced downward by a constant factor for clarity). This spectrum includes the OVII K α resonance line at 21.60 Å, which is easily detected at $z = 0$. The dotted line shows the location of the intergalactic absorption claimed by Nicastro et al. (2005) at $z = 0.011$.

and Galactic absorption. They treated separately the LETG/HRC data set, the LETG/ACIS data obtained by Nicastro et al. (2005), and the LETG/ACIS calibration observations. At the location of the strongest line reported by Nicastro et al. (2005), the OVII 21.60 Å line at $z = 0.011$, they confirm a dip in the spectrum in two of the three data sets. This feature was absent in the LETG/ACIS calibration observations (**Figure 7**). They fit the instrumental line spread function to the residuals of the normalized spectrum, rather than fitting a Gaussian. They find that only the LETG/ACIS spectrum obtained by Nicastro et al. (2005) shows a detection above the 2σ level (at 2.5σ), and only for the OVII line at $z = 0.011$. Their fit to both sets of data discussed by Nicastro et al. (2005) is 2.7σ , lower than the 3.8σ quoted by them, with the presumed difference being a result of the somewhat different fitting procedures.

Processing the *XMM-Newton* data poses several additional challenges because there are a number of features in the detector, such as hot pixels, which are not addressed when using the standard SAS processing. By using any recent version of the SAS (2006 or later), the resulting spectrum has several instrumental features seen in every bright spectrum. One of these happens to lie near 21.83 Å, which is very close to the OVII 21.60 Å line at $z = 0.011$ (21.85 Å), thus making it impossible

to determine its absorption line strength (Ravasio et al. 2005, Williams et al. 2006). However, if one constructs a complete map of all problematic pixels and uses that to define the acceptable data, it is possible to obtain high-quality spectra over nearly the entire *XMM-Newton* Reflection Grating Spectrometer (RGS) range, and that is the procedure used by Rasmussen et al. (2006). That effort describes the data processing and analysis of 955 ksec of RGS data from mid-2000 through late-2005, and by good fortune, Mrk 421 was quite bright during many of these observations. This led to a net spectrum where there were about 26,000 counts per 50 mÅ bin, about five times more than that used by Nicastro et al. (2005) in their *Chandra* data. Rasmussen et al. (2006) fit their RGS data similarly to the *Chandra* data and for the OVII line at $z = 0.011$. They find no detection. When they form a weighted average that includes the *Chandra* and *XMM-Newton* data, the line is a 1.0σ feature, well below the threshold for a detection.

Kaastra et al. (2006) argue that the statistical significance of the Nicastro et al. (2005) result should be reduced because they would have accepted an absorption at any wavelength over a redshift range of 0.03. As many instrumental resolution elements fit in this range, the statistical significance must include an appropriate number of trials, which is not considered in the discovery paper. We find the reanalysis and criticism by Kaastra et al. (2006) to be convincing and conclude that there is no statistically significant detection of intergalactic absorption in the OVII line toward Mrk 421. The rms of the *XMM-Newton* data is smaller than for the *Chandra* data, and the derived upper limit is $\log N(\text{OVII}) = 14.6$.

There is another claimed detection of absorption by the WHIM toward H1821+643. This is about an order of magnitude fainter in soft X rays than Mrk 421, but it is at $z = 0.297$, so there is more redshift range to search. It was observed for 470 ksec with the *Chandra* LETG/ACIS (Mathur et al. 2003), and the resulting spectrum had 2×10^5 photons, about 50 times less than the number of photons accumulated for Mrk 421 from all LETG observations. The observers searched for X-ray absorption that lay within 0.025 \AA of the redshifts of six intervening OVI absorption line systems determined from UV studies. They searched for absorption by OVII K α , OVIII K α , and NeIX K α , and they report one system associated with OVI absorption with a $S/N = 2.2$ and two systems with $S/N > 2$ that lie within $\pm 1000 \text{ km s}^{-1}$ of the OVI system (one in OVII K α and the other in OVIII K α). Given the ranges used by these investigators, there were effectively nine line resolution elements to find matches with the OVI systems and 20 trials for the matches near OVI systems. For the number of effective trials, finding a few 2σ absorption features has at least a 10% probability of occurrence according to our calculations. The more detailed error simulations of Kaastra et al. (2006) would suggest a higher probability of occurrence. These claimed features toward H1821+643 are not convincing detections either, and along with the failure of *XMM-Newton* to confirm the earlier *Chandra* result of Nicastro et al. (2005) in Mrk 421, lead us to conclude that the 10^6 – 10^7 K WHIM has not yet been detected beyond the Local Group.

In this ongoing search for the hot WHIM, there has been some confusion regarding the capabilities of the *Chandra* LETG compared to the *XMM-Newton* RGS. For example, it is often mentioned that the LETG has significantly higher resolution

than the RGS, which compensates for the difference in collecting area. This is a true statement at some wavelengths, because for a spectrally unresolved line where the continuum is well defined, the S/N of a detection is linearly proportional to the spectral resolution. However, it increases more slowly with the effective area, being proportional to its square root. At 21.6 \AA , the spectral resolutions are nearly the same for both observatories, being 0.05 \AA (FWHM) for the *Chandra* LETG and 0.06 \AA for the *XMM-Newton* RGS. Also, the wings of the line spread function contain more flux for the *XMM-Newton* RGS than for the *Chandra* LETG. In contrast, *XMM-Newton* has an effective area advantage of about a factor of 3–4, which more than compensates for the modest spectral resolution advantage of *Chandra*. For the particular case of Mrk 421, the *XMM-Newton* observations are about five times longer than the *Chandra* data used by Nicastro et al. (2005). Although the brightness during the *Chandra* observations approximately compensated for the collecting area difference of the two telescopes, the longer exposure time with *XMM-Newton* led to a spectrum with a lower rms.

The failure to detect the OVII line in the WHIM is not a problem for cosmological models (Cen & Fang 2005). The frequency of OVII absorption columns exceeding 10^{15} cm^{-2} is about $dN/dz \approx 1.5$ (Figure 8), so a Δz range of about 1 is needed for a reasonable chance of making a detection and Mrk 421 only offered $\Delta z = 0.03$.

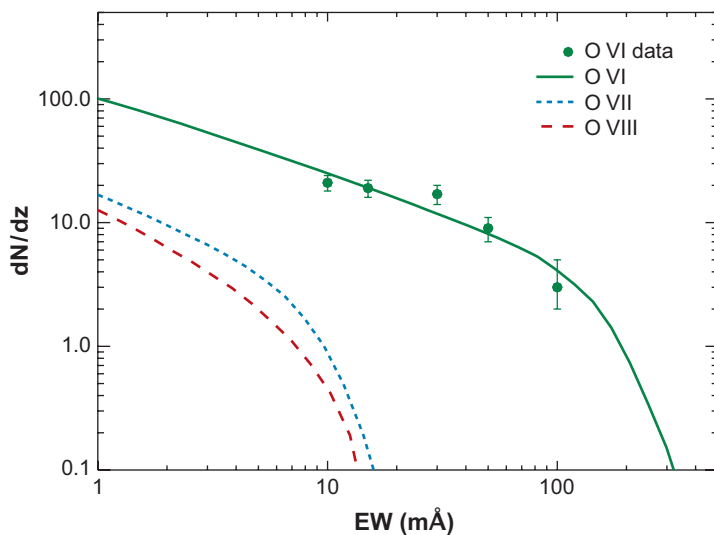


Figure 8

The differential number of absorbers as a function of equivalent width for OVI $\lambda 1035$, OVII $K\alpha$, and OVIII $K\alpha$, based on the model of Cen & Fang (2005). Absorption measurements from OVI (Danforth & Shull 2005) are in good agreement with the model. To detect the OVII and OVIII lines, one needs either path lengths of $\Delta z = 1$ and $\sigma < 2 \text{ m \AA}$, or shorter path lengths ($\Delta z = 0.1$) but $\sigma < 0.2 \text{ m \AA}$. This cannot be achieved with current instruments but should be achievable with future telescopes.

8. X-RAY EMISSION FROM THE WARM-HOT INTERGALACTIC MEDIUM IN AND NEAR GALAXY CLUSTERS

There has been much activity in the past decade in the effort to identify diffuse emission from the missing baryons both in and outside of galaxy clusters. The emission projected within the virial radius of galaxy clusters is discussed separately from the emission beyond the virial radius. Any emitting material must have a fairly high overdensity ($>10^2$), so even if it is truly detected, it is not the typical WHIM material predicted by models, but the upper density tail.

8.1. Soft Excess Emission Within the Virial Radius of Galaxy Clusters

Clusters of galaxies are among the brightest X-ray sources, containing hot gas (10^7 – 10^8 K) that accounts for more baryons than the visible galaxies (e.g., Allen et al. 2002). This gas has been studied at X-ray wavelengths for a variety of reasons, such as to determine the baryonic and gravitating mass or to study abundance patterns. The instruments used are spectroscopic imaging devices (proportional counters or CCDs) where each incoming photon can be assigned an energy to modest accuracy (3–50%, depending on the device and the photon energy). This permits one to carry out spatially-resolved spectroscopy, whereby a model spectrum is fit to the spectral energy distribution in some region, such as an annulus around the cluster center; the typical instrumental energy range is 0.2–10 keV. The spectrum is dominated by free-free radiation for typical cluster temperatures (3–10 keV), with line emission being of secondary importance. Another important parameter of the fit is the absorption by cool Galactic gas ($\leq 10^5$ K), as well as by material within the emitting source. This absorbing gas is due to the sum of the HI, H₂, and warm ionized gas at $\sim 10^4$ K, and as only the HI can be measured accurately, the absorption column is usually a fitted quantity, although with constraints. For typical column densities of 10^{20} – $10^{21.5}$ cm⁻², this absorption occurs at the low-energy part of the X-ray spectral energy distribution, 0.1–0.7 keV. Therefore, the simplest spectrum has a single temperature, abundance values, and absorption column density. If the simplest spectrum produces an unacceptable fit, more complicated fits are adopted. Unfortunately, there are several technical challenges, especially at the lowest energies, where instrumental calibration is most difficult and where background subtraction can pose problems.

The results of spectral fitting for galaxy clusters had led to claims of both excess absorption and excess emission. The claims about excess absorption began with spectra obtained with the *Einstein Observatory* SSS (Solid State Spectrograph) (White et al. 1991), where the soft emission was less than would be expected from a single-temperature cluster spectrum with Galactic absorption. This implied a significant amount of absorbing gas within the cluster. However, these SSS spectra had spectral corrections applied owing to the buildup of ice in the optical path. There was concern that if the correction for ice was wrong, the modified spectrum would have a soft X-ray deficit. This soft X-ray deficit was not confirmed with subsequent instruments,

such as *Rosat* (Arabadjis & Bregman 2000) or *XMM-Newton* (Peterson et al. 2003). We can safely conclude that the original study was incorrect and that there is no substantial absorbing medium within clusters.

Whether there is an additional emission component at soft X-ray energies (0.1–1 keV) has been a much more persistent and controversial subject. This line of study began with the detection of the Virgo Cluster by the *Extreme Ultraviolet Explorer* (EUVE), an instrument that was not designed to detect extragalactic objects. However, one of the imaging devices on the EUVE is the Deep Survey (DS) telescope (Bowyer & Malina 1991). It is sensitive to photons up to about 0.19 keV, the low-energy part of the soft X-ray region. At these energies, the optical depth is significant ($\tau = 3$ at 0.16 keV), but still small enough so that a modest amount of X-ray emission can pass through the gaseous Galactic disk and be detected by the EUVE. For a Galactic column density of $2 \times 10^{20} \text{ cm}^{-2}$, typical of high Galactic latitude sightlines, the effective bandpass of the EUVE is 0.144–0.186 keV (FWHM) but with a collecting area of only about 0.5 cm^2 (Bregman et al. 2003). Lieu et al. (1996) took the existing spectral fits to the X-ray data and asked whether the model also explained the EUVE measurement, but found that the model underpredicted the EUVE observations. They claimed that much of the emission detected by the EUVE was due to a new and previously unknown component of soft excess emission from galaxy clusters. One suggestion is that this soft excess emission is caused by nonthermal emission from cosmic rays in the galaxy clusters (Sarazin & Lieu 1998). However, if this soft excess is thermal, it would be due to gas at $1\text{--}3 \times 10^6 \text{ K}$, and the mass of gas involved must be comparable to the hotter ambient gaseous mass in the cluster (e.g., Kaastra et al. 2003). Therefore it would be of cosmological importance.

The claim of a soft excess detected with the EUVE was re-examined by the mission P.I., S. Bowyer, and collaborators. Berghöfer et al. (2000) argued that flat-fielding corrections were not properly applied to the EUVE data (see also Bowyer et al. 1999, 2001). They constructed flat fields from several very long observations and compared them to the same clusters for which excess emission had been claimed. They found that the flux detected by the DS on EUVE could be explained by a model that fit the cluster X-ray emission, but with no additional soft component; the only exception was the Coma cluster. In response to this work, Lieu et al. (1999) argued that there could be problems with using such a blank field, because time-dependent changes in the detector background would lead to analysis errors. Also, Lieu et al. (1999) suggested that the choice of threshold cutoffs in the pulse-height data could lead to incorrect results. These criticisms were considered and dispelled by Berghöfer et al. (2000), who found no evidence for time variation in the instrument's background and no significant effect due to the choices made in the pulse-height threshold level. In summary, with the exception of the Coma cluster, Bowyer and colleagues do not confirm the soft excess that Lieu and colleagues commonly detected.

Although it is remarkable that the EUVE was able to detect some galaxy clusters, it has far less collecting area than either *Rosat* or *XMM-Newton* in the same energy regions. The effective collecting area of the Deep Survey Lexan imager on EUVE is about an order of magnitude less than the collecting area of the *Rosat* PSPC (Position Sensitive Proportional Counters) or of the *XMM-Newton* EPIC pn (thin filter or open

position) for the same energy band and absorption conditions (Bregman et al. 2003). Therefore, most studies of the soft emission have concentrated on the soft X-ray observations of clusters. Some studies by Lieu and collaborators using the *Rosat* data showed that they were consistent with the EUVE data in that some fraction of the soft emission ($E < 0.5$ keV) required a new soft component in addition to the hotter cluster component (Lieu et al. 1996, Kaastra et al. 1999, Bonamente et al. 2001). These researchers also showed that the radial surface brightness profile of the soft excess was flatter than the surface brightness distribution of the hotter gas.

However, an examination of the *Rosat* data by Arabadjis & Bregman (1999) found that for annuli outside the central region, the cluster spectra could be fit with a single-temperature hot thermal spectrum plus Galactic absorption and that no additional soft component was needed. Again, the exception was the Coma cluster. The primary difference between this and the work where a soft excess was claimed has to do with the treatment of Galactic absorption. Rather than fixing the Galactic absorption at the 21-cm value, Arabadjis & Bregman (1999) permitted the value to vary within the uncertainties of the 21-cm measurement. The measurement of the 21-cm HI column is not straightforward because stray radiation can enter the radio beam and this has the greatest effect on sightlines out of the plane where the columns are smallest. It is possible to correct for this sidelobe contamination, but the uncertainties in those corrections and in the calibrations lead to the uncertainties in the 21-cm column (Hartmann et al. 1996, Murphy et al. 1996). Also, it was important to use the improved He absorption cross sections (Yan et al. 1998), because He is the primary absorber of soft X-rays at these columns.

There is likely to be a systematic effect in the absorption of soft X-rays, because of fluctuations in the Galactic interstellar medium. This systematic effect can cause an apparent soft excess (Bregman et al. 2003). The Galactic HI column is known to have small-scale structure and variations, yet when correcting for Galactic X-ray absorption in extended sources, one applies an average HI column measured from 21-cm emission. At low optical depth, it is sufficient to equate the X-ray absorption column to the mean column measured from 21-cm emission. However, at energies where there are moderate and high optical depths, such as the 0.15–0.5 keV region where investigators search for the soft excess, the X-ray absorption calculated from the mean HI column (as measured from 21-cm emission) leads to a systematically incorrect spectral fit. This can be seen if we consider two lines of sight with columns $N + \delta N$ and $N - \delta N$. The average would be N , which is what the 21-cm observer records, but the average fractional transmitted X-ray flux is $1/2\{\exp[-\sigma_E(N + \delta N)] + \exp[-\sigma_E(N - \delta N)]\}$, where σ_E is the absorption cross section at some energy. At low optical depth, the transmitted flux equals $F_o(1 - \sigma_E N)$, as though there were no column density fluctuations. However, when the optical depth exceeds unity, the above expansion is not accurate and the full exponentials must be retained. The extra radiation transmitted in the lower density line of sight is greater than the extra amount absorbed in the other line of sight so that the net transmitted flux is greater than if there were a single uniform column, i.e., $1/2\{\exp[-\sigma_E(N + \delta N)] + \exp[-\sigma_E(N - \delta N)]\} > \exp(-\sigma_E N)$. This effect leads to a correct fit at low optical depths but a positive residual at higher optical depths that would be interpreted as excess emission. To calculate the

magnitude of the effect, one would need an accurate map of the actual fluctuations in HI within the aperture being considered, and such data are not generally available. Instead, we estimate the effect based on N(HI) variations seen in other parts of the sky and find that it can be a contributor to the soft excess at moderate optical depths, typically for $N(\text{HI}) > 3 \times 10^{20} (E/0.3 \text{ keV})^3 \text{ cm}^{-2}$.

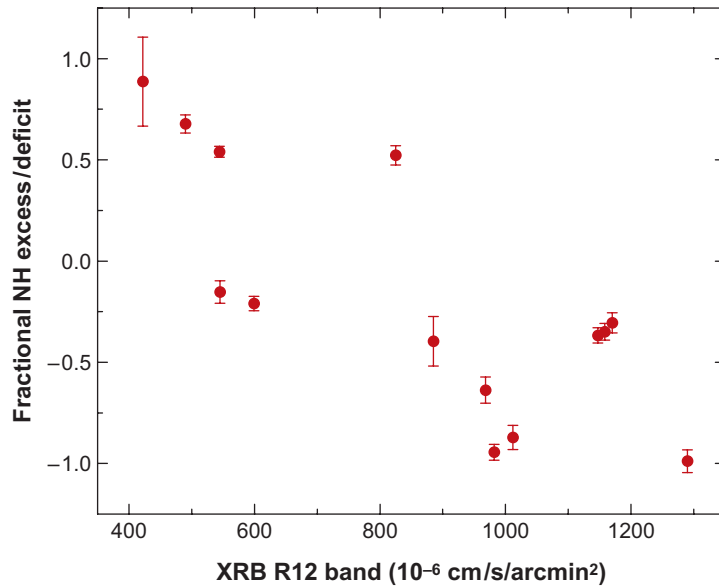
Following several studies with *Rosat*, the satellite *BeppoSAX* was used by Kaastra et al. (1999) to obtain data for Abell 2199 and to argue that it contains a soft component. In a rather forceful criticism of this work, Berghöfer & Bowyer (2002) examined the same data set but used a different approach to their analysis. They found no evidence for an additional soft component either in Abell 2199 or in Abell 1795, in agreement with the prior analysis for the same clusters by Arabadjis & Bregman (2000). In a rebuttal, Kaastra et al. (2002) argued that the analysis by Berghöfer & Bowyer was oversimplified, leading to their failure to detect the soft excess, which they reaffirm. The differences between these works once again have to do with the technical details of background subtraction and flat-fielding.

More recently, *Chandra* and *XMM-Newton* give us another opportunity to examine the problem. Owing to its larger field of view and lower energy response, *XMM-Newton* proves to be better-suited for this problem, so Kaastra et al. (2003) used *XMM-Newton* data to search for the soft X-ray excess emission in 14 galaxy clusters. When they adopted the Galactic HI column as the X-ray absorbing gas, a few clusters showed a soft X-ray deficit, which can be understood if there is additional gas along the line of sight, which, for example, could be due to molecular hydrogen. In the majority of the clusters, Kaastra et al. (2003) find evidence for excess soft emission and they show that it is broadly extended across the clusters. Several of the best cases are discussed in more detail, and they attribute some of the soft excess to emission from the OVII line. In addition, they point out that this line appears to be redshifted and is therefore not associated with the Galaxy or Local Group. The presence of OVII emission suggests that the emission mechanism is thermal and from a relatively cool component (0.1 keV) in or around the cluster, such as the WHIM.

The best cases showing a diffuse excess were examined separately by Bregman & Lloyd-Davies (2006), because they noticed that the strength of the soft excess emission seemed to correlate with Galactic latitude. A better correlation was found between the soft excess and the soft X-ray background near 1/4 keV [taken 5° from the cluster; the X-ray background used was the *Rosat* R12 bands of Snowden et al. (1994); this is in turn correlated with Galactic latitude; see also **Figure 9**]. Bregman & Lloyd-Davies (2006) suggested that the background subtraction method may have led to the soft excesses. The reason for this is that most of these clusters are too large for one to use a background from the same image. Therefore, Kaastra et al. (2003) used a standard background that had been compiled from a variety of observations around the sky, which represent an average X-ray background. Above 1 keV, the X-ray background is dominated by AGNs, and this component is fairly isotropic on the sky. However, below 1 keV, the X-ray background is dominated by the emission from Galactic gas and this emission can vary significantly around the sky. If the standard background below 0.5 keV is less than the Galactic value toward an individual cluster, then removal of the standard background inevitably results in an apparent soft X-ray excess.

Figure 9

The soft excess emission can be expressed as the fractional amount of HI that one would need to add to or remove from a spectral fit, assuming the ambient hot temperature for the cluster. Negative values indicate a soft excess. This quantity is strongly correlated with the Galactic 1/4 keV X-ray background, showing that the presence of an extra soft X-ray emission component is due to incorrect removal of the Galactic soft X-ray background (Bregman & Lloyd-Davies 2006).



To test this explanation, Bregman & Lloyd-Davies (2006) constructed backgrounds appropriate for each galaxy cluster by using backgrounds from other fields that had similar values for the Galactic soft background, $N(\text{HI})$, and the instrumental particle background (for clusters Abell 1795, Abell 1835, MKW 3s, and Abell S1101, also known as Sersic 159-03). When these individual backgrounds were subtracted from the observations of clusters, the resulting spectra could be fit without the need for an additional soft component. Also, Abell 1835 is small enough that an on-chip background can be used and the resulting spectrum did not show soft excess emission.

In summary, the reality of soft excess X-ray emission in galaxies has been seriously questioned, whether the data come from the EUVE, *Rosat*, *BeppoSAX*, or *XMM-Newton*. In every case, the disagreement can be traced to issues of flat-fielding (exposure maps) and background subtraction, which are tricky problems. Given the scientific importance of discovering the WHIM in galaxy clusters, we believe that the proponents of the soft X-ray excess must give unambiguous evidence for its presence. Until this is accomplished, the detection of the WHIM in galaxy clusters cannot be claimed.

8.2. The Coma Cluster

The Coma cluster is a possible exception in that the cluster spectrum appears to require extra emission at low energies (<0.4 keV) even if one uses a Galactic HI column near the low end of its likely range (in this direction, $N(\text{HI}) = 0.9 \pm 0.1 \times 10^{20} \text{ cm}^{-2}$). All investigators agree that an excess is present in this cluster, with the most recent work in X rays by Finoguenov et al. (2003), who use *XMM-Newton* data. They use a background from another part of the sky, which they scale to

the HI column appropriate for the Coma cluster. This has the shortcoming that the soft X-ray background varies around the sky, as does the fraction from the Galactic halo and the Local bubble, so there is no unique method for scaling the background from one region to another. It is not possible to use a local background because the virial radius of Coma (assumed to be 3 Mpc) is 1.7° , much larger than the field of view of the EPIC camera. Given these shortcomings, these researchers have performed a careful analysis and in their resulting spectrum, they detect the OVII and OVIII features, from which they obtain a redshift of $0.007 \pm 0.004 \pm 0.0015$ (best-fit, statistical, and systematic error). This is within 1.3σ of zero redshift, expected for Galactic emission, but it is about 3σ from the redshift of the Coma cluster, 0.023. In support of soft emission from Coma, there are weak Ne IX and OVIII absorption lines at 2.3σ and 1.9σ , obtained with the RGS on *XMM-Newton* (Takei et al. 2007). If these could be confirmed, it would be strong support of cooler material around the Coma cluster.

There are three possible explanations for this apparent excess. The first is that the Galactic soft X-ray background happens to be high in this direction because of the properties of Galactic gas. The Galactic HI column lies in a local minimum in this direction (very close to the North Galactic Pole), which certainly was not caused by the Coma cluster. A minimum in $N(\text{HI})$ should let more Galactic halo emission through, leading to a brightening that is unrelated to the Coma cluster. Such brightenings in the 1/4 keV band are seen in other directions of low HI, including the Lockman Hole. This local hole near the Coma cluster can be seen in the dust extinction map (**Figure 10**) that utilized the IRAS and COBE data (Schlegel et al. 1998). The typical extinction about 4° from the center of Coma is about 0.015 magnitudes. Even this is several times smaller than the typical sightline out of the Galaxy. However, the Coma cluster lies in a region where the extinction is more typically 0.008–0.009, an extremely low value.

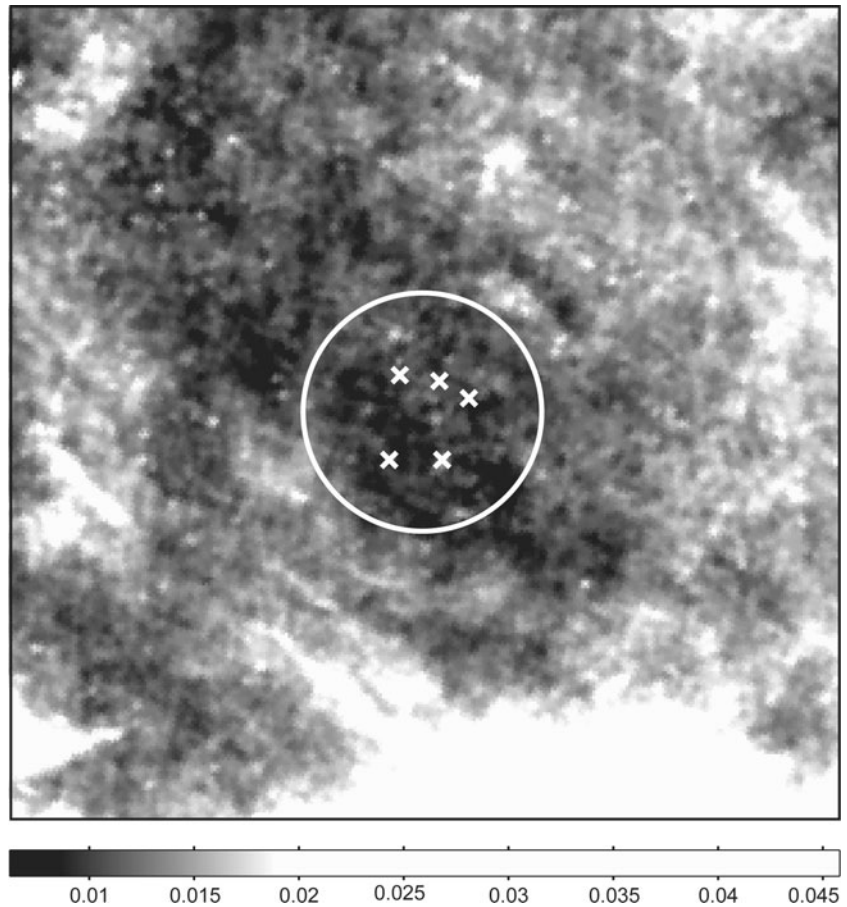
A related possibility is that $N(\text{HI})$ is actually lower than measured because the sidelobe contamination has been underestimated, an issue that is worst for the lowest columns (Hartmann et al. 1996, Murphy et al. 1996). With a mean column of $6\text{--}7 \times 10^{19} \text{ cm}^{-2}$, a spectral model does not require a soft excess component, but this value lies about 3σ below current measurements for the HI column in this direction.

The third possibility is that there is a soft component and that it is produced by inverse Compton scattering of the CMB by energetic particles in the cluster. Such a possibility is attractive because this is one of the only clusters with a bright nonthermal radio halo. This model was suggested previously (Sarazin & Lieu 1998), but Bowyer et al. (2004) argue that the EUV and the X-ray emission fall more steeply than expected if the nonthermal electron density decreased as the hot gas density. A steeper decrease in the nonthermal particles is implied, so Bowyer et al. (2004) argue that the nonthermal particles responsible for scattering photons are secondaries caused by interactions of the cosmic ray primaries with the hot gas.

To summarize, there appears to be an excess of soft X-ray emission from the direction of the Coma cluster, but it may not be from a $\sim 10^6$ K medium within the cluster. The soft X-ray excess could have a Galactic origin or it may be due to nonthermal processes within Coma. Higher quality X-ray spectral observations could help to clarify the matter.

Figure 10

The dust extinction map of the Coma cluster region (from Schlegel et al. 1998), in units of magnitudes of extinction. A circle of 3 Mpc radius (1.7°) is centered on the Coma cluster. The crosses show the locations of the regions used by Finoguenov et al. (2003) to determine the properties of an X-ray filament. The Coma cluster happens to lie in a region of particularly low extinction, which may let through additional Galactic halo emission that could be mistaken for a feature intrinsic to Coma.



8.3. The Absence of OVI Emission

The soft diffuse emission has been interpreted as being caused by thermally emitting gas with a temperature in the range $0.5\text{--}1 \times 10^6$ K, which is close to the peak of the cooling function. Unless balanced by an unknown heating mechanism at this temperature, the gas should continue to cool through the 3×10^5 K range, where most of the thermal energy is emitted through the OVI $\lambda\lambda$ 1032 1038 lines. This emission is accessible with certain extreme UV spectroscopic instruments, notably the *Hopkins Ultraviolet Telescope* (HUT) and FUSE (Dixon et al. 1996, 2001), the latter having better sensitivity. Five clusters were observed with HUT: the Hercules cluster, Abell 1795, Abell 1367, the Coma cluster, and the Virgo cluster. Only upper limits were obtained to the OVI emission, which were inconsistent with the presence of 5×10^5 K gas in the Virgo cluster. Their more recent FUSE observations of the Virgo and Coma clusters (Dixon et al. 2001) are significantly deeper. They also fail to detect the OVI emission. These observations rule out all published models in which the soft excess is caused by thermal emission in these galaxy clusters. The absence of

the OVI emission further brings into question the presence of WHIM material in the Coma and Virgo clusters.

8.4. X-Ray Emission Beyond the Virial Radius of Galaxy Clusters

In principle, a successful emission study of the WHIM could measure the temperature, intensity, metallicity, and, most importantly, the topology of the gas (expected to be a web of connected filaments). In practice, this is challenging because one is observing a volume emission measure that is expected to be much fainter than galaxy clusters or even galaxy groups. For a typical rich cluster where X-ray emission is easily detected, a representative density is $n_e \approx 3 \times 10^{-4} \text{ cm}^{-3}$, or $\rho_{\text{gas}}/\langle\rho_{\text{gas}}\rangle \approx 1500$. The density is falling roughly as r^{-2} , so at double the radius the gas density has dropped by a factor of four but the emission measure has decreased by more than an order of magnitude and is becoming very difficult to detect (for $\rho_{\text{gas}}/\langle\rho_{\text{gas}}\rangle < 500$). The typical overdensity in the WHIM is 10^0 – 10^3 and for gas above 10^7 K (typical of groups and clusters), it is 10^2 – 10^4 . So if one were to detect most of the mass of the WHIM, it would be necessary to reach overdensities of 10, about 2000 times lower surface brightness than currently detectable limits. In addition, for clusters or groups, one can obtain a brightness in an annulus, improving photon statistics, in contrast to filaments where the location, shape, and extent are unknown. An additional reduction in the surface brightness would occur if the metallicity in the filaments is lower than in galaxy clusters, because most of the emission is from metal lines at these temperatures.

Aside from the issue of the soft excess from clusters, where the presence or absence is often due to the method used to flat-field the data, there are other efforts to detect this emission.

Emission from the WHIM with temperatures below about 0.1 keV should be impossible to detect owing to Galactic absorption, so the part of the WHIM that one seeks to detect is hotter, in the 10^6 – 10^7 K range. As there is a weak correspondence between temperature and overdensity, gas in this temperature regime would have a characteristic overdensity of $10^{2 \pm 1}$.

There have been several investigations of the emission around and between galaxy clusters. Using *Rosat* data, which provides a larger field of view than any current instrument, Soltan et al. (1996) argued that Abell clusters have extended low surface brightness halos that extend to a characteristic radius of 7 Mpc, about twice the virial radius. However, Briel & Henry (1995) searched for filaments connecting 54 Abell clusters, with separations of 4–17 Mpc. Hierarchical clustering theory predicts that the emission from the WHIM should be brightest along loci between clusters, but Briel & Henry failed to detect emission. For a temperature of 1 keV ($1.2 \times 10^7 \text{ K}$), a metallicity of 0.3 of the Solar value, and a filament width of 0.5 Mpc, their 3σ upper limit to the electron density is $9 \times 10^{-5} (l/0.5 \text{ Mpc})^{-1} \text{ cm}^{-3}$, where l is the assumed thickness of the filament. For a temperature of 0.5 keV ($6 \times 10^6 \text{ K}$) and a metallicity of 0.1 Solar, the density limit would be twice as large. These upper limits still represent an overdensity of 400–1000, so the failure to detect such filaments is not in conflict with model predictions.

Searches for filaments were made using pointed *Rosat* PSPC data and Scharf et al. (2000) have claimed the detection of a filament at about the 3σ level. Its surface brightness is about three times lower than the limit of Briel & Henry (1995), corresponding to an electron density that is about a factor of two lower. There are some concerns with this result, acknowledged by the investigators. For example, the cluster is superimposed on one of the brightest regions in the Galactic soft 1/4 keV X-ray background. Although Scharf et al. (2000) work in the 0.5–2 keV band, the plasma responsible for the Galactic 1/4 keV background also has strong OVII emission at 0.58 keV, so much of this would fall in their band. Without more detailed spectral information, it will be difficult to tell whether this filament is related to structure in the Galactic soft X-ray background or whether it is intrinsic to the CL 1603 field.

A search for filamentary connections between clusters in the Shapley supercluster was undertaken by Kull & Böhringer (1999). *Rosat* data were used to analyze a 6° by 3° region containing three luminous central clusters (Abell 3562, Abell 3558, and Abell 3556). About 1.5 Mpc between Abell 3558 and Abell 3556, dilute emission was detected and it is softer than the bright cluster emission, consistent with gas in the 0.5–1 keV range. The surface brightness is about twice the 3σ limit of Briel & Henry (1995). This appears to be a strong detection. However, the projected position places this within the virial radius of both clusters, making it difficult to claim that this is an unvirialized filament of moderate density.

More recently, *XMM-Newton* data were used to investigate an extended 4 Mpc filament near Abell 85 that was originally discovered with the *Rosat* PSPC (Durret et al. 2003). They confirm the *Rosat* result and show that the extended feature has the same position angle as the major axis of the central cD, the cluster galaxies, and the nearby galaxy clusters groups. The temperature of the filament was measured to be 2 keV (2.5×10^7 K), and although this is cooler than the clusters, it is significantly hotter and brighter than expected for the WHIM. Also, its projected length extends only a bit beyond the virial radius of Abell 85 (about 3 Mpc), so this may be interacting with the cluster, as the researchers suggest (among other possibilities).

One of the greatest challenges in this sort of work is removing the instrumental background, which can be larger than the net signal. In that regard, the newest X-ray telescope, *Suzaku*, is advantageous in that it has a lower soft X-ray instrumental background than previous missions. The spectral resolution of the CCD also is improved, allowing studies in narrow wavelength bands that focus on emission from particular ions, such as OVII. Among the first investigations is a search for OVII and OVIII emission around the cluster Abell 2218 (Takei et al. 2007). They examine regions 10–20 Mpc from the cluster center but do not detect excess emission. Their limiting value is about a factor of five below previous claims of soft excess emission (Kaastra et al. 2003). Their density limit is $n_H < 7.8 \times 10^{-5} \text{ cm}^{-3}$ for $Z = 0.1 Z_\odot$ and a path length of 2 Mpc. This corresponds to an overdensity of 270, which is still higher than the typical predicted overdensity of the WHIM, so this upper limit is consistent with expectations.

In conclusion, although there does appear to be faint emission at about the virial radius of rich clusters, there is no definitive detection of a filament that is well beyond the virial radius that has a temperature of 10^6 – 10^7 K.

8.5. Shadowing the Diffuse Component of the X-Ray Background

Rather than detect faint filaments directly, another approach is to detect the sum of many filaments. This has the advantage that the surface brightness should be many times greater than a single filament, especially because some filaments will be seen along their long axis. There have been calculations of the expected surface brightness and the angular fluctuations around the sky (Croft et al. 2001, Voit et al. 2001). The emission is dominated by multiple lines of Fe (L series) and O (OVII and OVIII) for abundances above 0.01 of the Solar value. The important lines lie below 1 keV and there are two selection effects that lead to the emission being confined to the 0.2–1 keV range. Emission below 0.2 keV is absorbed by the Milky Way and the Galactic X-ray background is bright below about 0.4 keV. Therefore, emission from high redshift gas will be redshifted into these unfavorable energy ranges. Also, at higher redshifts, the fraction of WHIM gas decreases, leading to less emission. Calculations of the cumulative emission show that it should be most prominent around 0.7 keV with a moderate range, so a useful band is 0.4–1.0 keV. The emission-weighted mean redshift is $\langle z \rangle = 0.32$ (Cen et al. 1995) and the peak effective temperature is about 3×10^6 K (Croft et al. 2001).

In this energy band, three components contribute to the diffuse X-ray background: the Galactic soft background, unresolved AGNs, and the WHIM. The WHIM is expected to be the minority component, contributing at the 1–10% level, although this prediction is model-dependent (Cen et al. 1995, Croft et al. 2001, Phillips et al. 2001). A very important nonastronomical component is the background caused by the instrument and by material in the Solar System (cosmic rays, scattered Solar X rays, etc.). Usually, this is comparable to the astronomical diffuse background and it varies in time. Separating these many components and extracting the small component of the WHIM is challenging and can only be accomplished under special circumstances or with a specially designed (future) mission.

One of the special situations in which instrumental backgrounds can be removed is the *Rosat* All-Sky Survey (RASS), where there are many overlapping and continuous fields. By using the anticorrelation between the RASS and the Galactic HI survey, Kuntz & Snowden (2000) were able to separate local emission from emission beyond the HI layer. They modeled the emission beyond the HI layer with two thermal components at 1.1×10^6 K and 2.9×10^6 K. This emission contains all sources beyond the disk, including unresolved point sources. Based on deep point-source studies, they removed these components and arrived at a uniform all-sky value of $7.5 \text{ keV s}^{-1} \text{ cm}^{-2} \text{ sr}^{-1} \text{ keV}^{-1}$ in the 3/4 keV band (Kuntz et al. 2001). Some portion of this emission is probably associated with the Galactic halo, which could be the dominant component. This value constitutes the upper limit to the 3/4 keV emission from the WHIM. It is comparable to the value of $7 \text{ keV s}^{-1} \text{ cm}^{-2} \text{ sr}^{-1} \text{ keV}^{-1}$ suggested by Cen & Ostriker (1999), but an order of magnitude larger than the estimate of Phillips et al. (2001) for the WHIM.

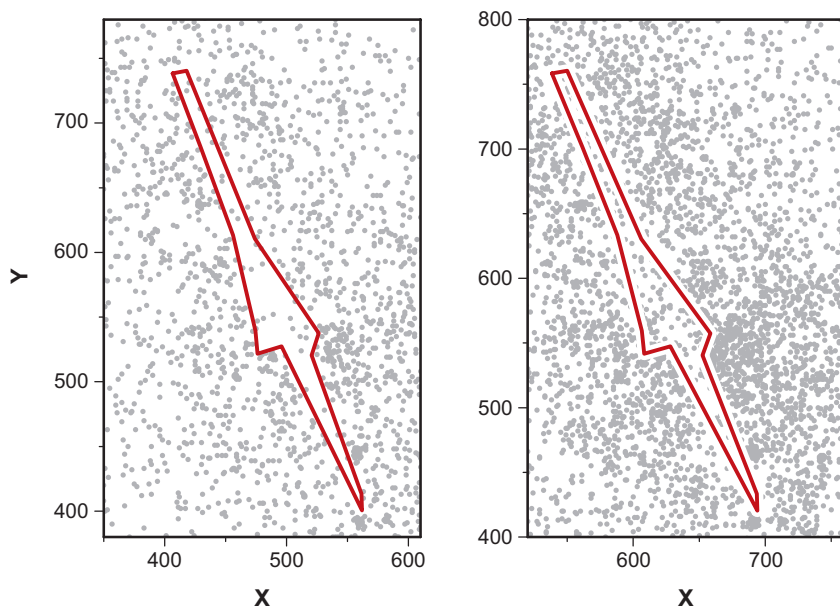
A method of directly determining the extragalactic background, separated from other backgrounds, is through X-ray shadowing. The technique uses a cloud that lies at some interesting distance and for which the opacity due to photoelectric absorption

is significant enough to be measured. A spatially large diffuse emission component behind the cloud will appear less bright at the cloud location because of absorption by the cloud. That is, the cloud produces a shadow. This was used successfully to demonstrate that a significant amount of the 1/4 keV diffuse background lies beyond the Local bubble. It can also be used to shadow the diffuse emission from the WHIM, provided that sufficiently dense clouds lie beyond the Local Group. Spiral galaxies have the requisite amount of cold gas but they also contain emitting sources (X-ray binaries, supernova remnants, etc.). Therefore, it is necessary to find a situation where the emitting sources are unimportant. Such a situation can occur for edge-on galaxies, either because gas extends beyond the disk of stars or because the column density of gas is so large in the disk that it absorbs essentially all of the emission from sources in the galaxy. This approach is made easier with *Chandra* as one can identify and exclude point sources to good accuracy.

The edge-on galaxy NGC 891 would appear to be a suitable object for this approach. Bregman & Irwin (2002) used the high optical (and X-ray) extinction region of the midplane of NGC 891 for shadowing; this region subtends less than 1 square arcminute. Aside from disk point sources, the galaxy has some halo emission and if this is on a scale larger than the HI disk, the shadowing approach would not work. Bregman & Irwin (2002) reported a possible detection of a shadow. In the extinction region, 68.4 photons were expected but only 51 photons were detected, which is a deficit that would be expected to occur only 1.7% of the time. However, in a subsequent and significantly longer observation, the shadow was not confirmed (J.N. Bregman, in preparation; **Figure 11**). The upper limit provided by this observation is less restrictive than that of Kuntz et al. (2001).

Figure 11

Two *Chandra* images of NGC 891 in the energy band 0.4–1.0 keV, where the region of high optical extinction is delineated by the red polygon. Each pixel is 0.5 arcsec, so the field is 3.3 arcsec high and each dot is a single photon. The X-ray shadow seen in the first observation (*left*, Bregman & Irwin 2002) is not confirmed with more recent data (*right*).



9. OTHER TECHNIQUES FOR DETECTING THE WARM-HOT INTERGALACTIC MEDIUM

Although this review has focused on the X-ray and UV absorption lines as the primary tools for detecting the WHIM, there are other promising techniques. Most will require instrumental improvements to be competitive. However, as there are plans for significant instrumental improvements in the future, they could become important new approaches for WHIM studies.

9.1. Dispersion Measures

An ionized plasma has a frequency-dependent index of refraction, which produces a measurable effect at radio wavelengths. The effect is well-known and used to study pulsars: the pulse at lower frequencies lags the same pulse observed at higher frequencies. The difference of the arrival times of the same pulse at different frequencies is proportional to the dispersion measure, which is the integral of the electron density over the path length. The electron column density is precisely the quantity that one would like to measure through cosmological space. From it, one can determine the mass content of the WHIM without the abundance or ionization corrections that must be confronted with most other methods. The dispersion measure has been measured through the Milky Way as well as for pulsars projected upon the Magellanic Clouds, and the total electron column out of the Milky Way is about $5 \times 10^{19} \text{ cm}^{-2}$ (Taylor & Cordes 1993, Cordes 2001, Crawford et al. 2001). This is similar to the column inferred from the OVII K α absorption (Bregman & Lloyd-Davies 2007).

The 20 pulsars in the Small and Large Magellanic Clouds have dispersion measures that are several times the value associated with the Milky Way (Manchester et al. 2006). Also, these dispersion measures vary by up to a factor of five between pulsars. Both the high values and the variation are attributed to the ionized interstellar gas in the Magellanic Clouds. The expected dispersion measure from diffuse gas between the Milky Way and the Magellanic Clouds is less than the variation between the Magellanic Cloud pulsars. This prevents one from using them to gain information about halo or Local Group gas.

Unfortunately, pulsars have not been detected beyond the LMC, so we cannot use this approach to determine the total electron column in the Local Group or beyond. Studies of AGNs have failed to find pulses or other variations on a sufficiently short timescale to be used to determine dispersion measures over cosmological distances. Another class of candidates are gamma-ray bursters, provided that they have sufficiently sharp prompt radio emission. Ioka (2003) has examined this possibility and discusses its feasibility with a future instrument such as the Square Kilometer Array. One problem with using either AGNs or gamma-ray bursters for dispersion measure determinations is that the environment of these objects may produce dispersion measures in excess of the cosmological values.

9.2. Radio Hyperfine Lines

Another approach may be provided by using the hyperfine lines of highly ionized species. These would be equivalent to the 21-cm hyperfine transition for hydrogen.

They occur in either hydrogenic or lithium-like species with significant nuclear magnetic moments (Sunyaev & Churazov 1984). Unfortunately, most of the common elements are composed of alpha particles, which have weak magnetic moments and do not produce useful hyperfine lines. Nitrogen is one of the only exceptions to this rule because it is made in abundance through the CNO process. A hyperfine line occurs at 53.2 GHz in hydrogenic nitrogen (NVII), but the Earth's atmosphere is opaque at this frequency. Because of this, the line cannot be used to probe the Local Group, but it can be used at modest redshift ($z > 0.1$) where the atmosphere is transparent. In this line, the emission from the WHIM is too small to be detectable, but the detection of this line in absorption holds promise (Goddard & Ferland 2003). For HI, the hyperfine absorption feature is greatly reduced by stimulated emission, because the two levels are close to their Boltzmann ratio and the collision time is much shorter than the lifetime of the excited level. However, for NVII, the transition time is less than the time between collisions for WHIM conditions, so stimulated emission is less important and NVII is a much better absorber.

The NVII hyperfine line can be compared to the OVII $K\alpha$ absorption, where a column of 10^{16} cm^{-2} yields a good absorption feature. Nitrogen is six times less common, so the central optical depth of the line, which is easily resolved with radio receivers, is $< 10^{-3}$. For a good detection, it would be necessary to achieve opacities of 10^{-4} or less. One difficulty is that few continuum sources are strong in the 40–50 GHz range, but there are several sources brighter than a few Janskies. We observed several radio-loud AGNs to search for such weak lines in 3C 273, 3C 279, 3C 345, and 4C 39.25 (J.N. Bregman & J.A. Irwin, submitted). Although no absorption features were discovered above the 5σ level, these observations showed that it was possible to obtain an rms per channel as low as 10^{-4} with about an hour of integration. For integration times of 25–30 hours on the brightest objects, the sensitivity is comparable to 300-ksec X-ray observations of the brightest sources, provided that the rms of the radio spectrum continues to decrease as the inverse square root of the integration time. Radio observations have their own set of systematics problems, such as standing waves, but these systematics are different from the X-ray observations, so radio studies provide a valuable complement in the search for the WHIM.

A variety of other hyperfine lines are available for study, but as Goddard & Ferland (2003) point out, nearly all of the others are too rare to have any likelihood of being detectable in absorption by the WHIM.

9.3. The Sunyaev-Zel'dovich Effect and the Warm-Hot Intergalactic Medium

The passage of the CMB through a hot cloud of electrons causes the photons to gain energy, leading to a distortion of the spectrum [the Sunyaev-Zel'dovich (S-Z) effect]. At frequencies below about 200 GHz, this leads to an apparent decrease in the temperature of the CMB, and the magnitude of the shift is proportional to the line integral of the pressure of the hot medium. The effect is seen in rich clusters of galaxies (Grego et al. 2001), and even in the survey data from the first year of the *Wilkinson*

Microwave Anisotropy Probe (WMAP), it is detected (Hernández-Monteagudo et al. 2004).

In practice, there should be a S-Z effect caused by the WHIM in the form of filaments. Relative to clusters, the temperature in the WHIM is at least an order of magnitude lower and the column density through a filament is also at least an order of magnitude smaller. Therefore, the S-Z effect in WHIM filaments should be at least two orders of magnitude smaller than for rich clusters. Hansen et al. (2005) searched for such a signal by using galaxies to trace WHIM filaments, which they correlated with *WMAP* data. They conclude that the S-Z signal from the WHIM cannot be detected with the current *WMAP* data and they derive upper limits.

Although direct detection of WHIM filaments may be out of reach at the moment, it may be possible to probe the outer parts of clusters and groups. However, this is challenging as well. Hernández-Monteagudo et al. (2004) searched for but failed to see a S-Z signal from structures less bound than clusters. Myers et al. (2004) report on a similar study that used the same *WMAP* data in which they have a marginal detection of the S-Z effect on a size scale (5 Mpc) somewhat greater than the virial radius of the cluster. Given the disagreement between the groups and the marginal detection by Myers et al. (2004), the evidence is not compelling that the S-Z effect has been detected beyond the virial radius of galaxy clusters. However, future instruments may provide enough improvements in sensitivity to make such studies feasible.

10. FINAL COMMENTS AND FUTURE PROSPECTS

The search for the WHIM is a relatively new field in which the majority of studies are pioneering efforts that are technically challenging. We can look at the final census and try to anticipate where future instrumentation might make the greatest impact. The combination of the stars and gas in galaxies, galaxy clusters, and galaxy groups accounts for about 12% of the baryons. The gas that produces Ly α absorption at low redshift accounts for about 30–50% of the baryons ($T \times 10^5$ K). Of the remaining material, there is a secure detection of WHIM material in the temperature range $1\text{--}5 \times 10^5$ K through the OVI absorption lines seen in a number of lines of sight, and this comprises about 7% of the baryons. The remaining 30–50% of the baryons are predicted to lie in the temperature range between $0.5\text{--}30 \times 10^6$ K. Although there have been many claims for the detection of cosmologically significant amounts of gas in this temperature range, these results are not compelling. We define a compelling detection as one that is above 5σ , that is confirmed by multiple instruments (when appropriate), and does not disappear for different choices of data reduction procedures (such as using different backgrounds or flattening procedures).

Gas near 7×10^5 K can be studied if the redshifted resonance lines from Li-like NeVIII λ 773 can be detected. The equivalent widths of these lines are about an order of magnitude less than the OVI λ 1035 lines, so with sufficiently long observations with FUSE or HST (with the Cosmic Origins Spectrograph), it might be possible to detect this species above the 5σ level (a 3.9σ detection is currently claimed; Savage et al. 2005). Above this temperature, progress requires X-ray observations, typically from the resonance lines of hydrogenic or He-like species, such as OVII and OVIII.

The OVII $K\alpha$ line is the most promising diagnostic at temperatures near 10^6 K, whereas the OVIII $K\alpha$ line is most common in gas at $10^{6.35}$ K but with a wide temperature range (up to about 5×10^6 K). These species have been detected in absorption at zero redshift. This absorption is most likely caused by Galactic halo gas, which is not massive enough to be of cosmological importance. There is no compelling evidence for absorption by these ions from intergalactic gas. This is not in conflict with models, which show that about an order of magnitude greater sensitivity is needed along several lines of sight in order to detect such absorption. This improvement in sensitivity is provided by the present design of *Constellation-X*, which should usher in a rich period of discovery for WHIM studies. Studies of absorbing gas at 10^7 K and above require using species such as MgXII (the $K\alpha$ line), which are at least an order of magnitude less common than oxygen and where the absorption line occurs at higher energies. Detecting these absorption lines will be challenging.

We conclude that there is no compelling evidence for emission from WHIM material within clusters or beyond the virial radius. The most important observations would be detecting the WHIM beyond the virial radius. This would reveal the shape and amplitude of the cosmic web of baryons. Any observation along these lines must demonstrate that the gas is at the expected redshift, and this requires sensitive spectroscopic observations with very low instrumental noise and a moderately broad field of view. This cannot be achieved with current instrumentation, but is perfectly feasible with future wide-field instruments using quantum microcalorimeters.

Finally, there are other technologies that may prove useful, such as S-Z measurements and radio NVII absorption line observations. The S-Z measurements are most sensitive to hotter gas, as the signal is caused by the pressure integral along one's line of sight, so it would nicely complement X-ray absorption line observations. However, at least one order of magnitude improvement in sensitivity will be required for this approach to be feasible.

Uncovering the missing baryons is a feasible goal, requiring only sensitivity improvements that can be attained with existing technologies. We hope that these sensitivity improvements will be realized in the coming decade through the construction of the next generation of instruments. The result would be a flood of new discoveries.

DISCLOSURE STATEMENT

The author is not aware of any biases that might be perceived as affecting the objectivity of this review.

ACKNOWLEDGMENTS

I would like to thank Jon Miller, Jimmy Irwin, Renato Dupke, Mary Putman, Ken Sembach, and Pat Henry for many helpful conversations. Also, Andy Rasmussen and Fabrizio Nicastro helped to clarify some technical issues. I would like to acknowledge support from NASA through the LTSA grant program.

LITERATURE CITED

- Allen SW, Schmidt RW, Fabian AC. 2002. *MNRAS* 334:L11
- Arabadjis JS, Bregman JN. 1999. *Ap. J.* 514:607
- Arabadjis JS, Bregman JN. 2000. *Ap. J.* 536:144
- Berghöfer TW, Bowyer S. 2002. *Ap. J. Lett.* 565:L17
- Berghöfer TW, Bowyer S, Korpela E. 2000. *Ap. J.* 545:695
- Blitz L, Robishaw T. 2000. *Ap. J.* 541:675
- Bonamente M, Lieu R, Mittaz JPD. 2001. *Ap. J.* 546:805
- Bowyer S, Berghöfer TW, Korpela EJ. 1999. *Ap. J.* 526:592
- Bowyer S, Korpela E, Berghöfer T. 2001. *Ap. J. Lett.* 548:L135
- Bowyer S, Korpela EJ, Lampton M, Jones TW. 2004. *Ap. J.* 605:168
- Bowyer S, Malina RF. 1991. *Adv. Space Res.* 11:205
- Bregman JN, Irwin JA. 2002. *Ap. J. Lett.* 565:L13
- Bregman JN, Lloyd-Davies EJ. 2006. *Ap. J.* 644:167
- Bregman JN, Lloyd-Davies EJ. 2007. *Ap. J.* In press
- Bregman JN, Novicki MC, Krick JE, Arabadjis JS. 2003. *Ap. J.* 597:399
- Briel UG, Henry JP. 1995. *Astron. Astrophys.* 302:L9
- Bristow PD, Phillipps S. 1994. *MNRAS* 267:13
- Cen R, Fang T. 2006. *Ap. J.* 650:573
- Cen R, Kang H, Ostriker JP, Ryu D. 1995. *Ap. J.* 451:436
- Cen R, Ostriker JP. 1999. *Ap. J.* 514:1
- Cen R, Ostriker JP. 2006. *Ap. J.* 650:560
- Connors TW, Kawata D, Gibson BK. 2006. *MNRAS* 371:108
- Cordes J. 2001. *Ap. Space Sci.* 278:11
- Crawford F, Kaspi VM, Manchester RN, Lyne AG, Camilo F, D'Amico N. 2001. *Ap. J.* 553:367
- Croft RAC, Di Matteo T, Davé R, Hernquist L, Katz N, et al. 2001. *Ap. J.* 557:67
- Danforth CW, Shull JM. 2005. *Ap. J.* 624:555
- Davé R, Cen R, Ostriker JP, Bryan GL, Hernquist L, et al. 2001. *Ap. J.* 552:473
- Dixon WVD, Hurwitz M, Ferguson HC. 1996. *Ap. J. Lett.* 469:L77
- Dixon WVD, Sallmen S, Hurwitz M, Lieu R. 2001. *Ap. J. Lett.* 550:L25
- Durret F, Lima Neto GBL, Forman W, Churazov E. 2003. *Astron. Astrophys.* 403:L29
- Fang T, Mckee CF, Canizares CR, Wolfire M. 2006. *Ap. J.* 644:174
- Finoguenov A, Briel UG, Henry JP. 2003. *Astron. Astrophys.* 410:777
- Fukugita M, Hogan CJ, Peebles PJE. 1998. *Ap. J.* 503:518
- Fukugita M, Peebles PJE. 2004. *Ap. J.* 616:643
- Goddard WE, Ferland GJ. 2003. *PASP* 115:647
- Grego L, Carlstrom JE, Reese ED, Holder GP, Holzapfel WL, et al. 2001. *Ap. J.* 552:2
- Hansen FK, Branchini E, Mazzotta P, Cabella P, Dolag K. 2005. *MNRAS* 361:753
- Hartmann D, Kalberla PMW, Burton WB, Mebold U. 1996. *Astron. Astrophys. Suppl.* 119:115
- Hernández-Monteagudo C, Genova-Santos R, Atrio-Barandela F. 2004. *Ap. J. Lett.* 613:L89
- Ioka K. 2003. *Ap. J. Lett.* 598:L79

- Jansen F, Lumb D, Altieri B, Clavel J, Ehle M, et al. 2001. *Astron. Astrophys.* 365:L1
 Kaastra JS, Lieu R, Bleeker JAM, Mewe R, Colafrancesco S. 2002. *Ap. J. Lett.* 574:L1
 Kaastra JS, Lieu R, Mittaz JPD, Bleeker JAM, Mewe R. et al. 1999. *Ap. J. Lett.*
 519:L119
 Kaastra JS, Lieu R, Tamura T, Paerels FBS, den Herder JW. 2003. *Astron. Astrophys.*
 397:445
 Kaastra JS, Werner N, den Herder JWA, Paerels FBS, de Plaa J, et al. 2006. *Ap. J.*
 652:189
 Kang H, Ryu D, Cen R, Song D. 2005. *Ap. J.* 620:21
 Kauffmann G, Heckman TM, White SDM, Charlot S, Tremonti C, et al. 2003.
MNRAS 341:33
 Kull A, Böhringer H. 1999. *Astron. Astrophys.* 341:23
 Kuntz KD, Snowden SL. 2000. *Ap. J.* 543:195
 Kuntz KD, Snowden SL, Mushotzky RF. 2001. *Ap. J. Lett.* 548:L119
 Lieu R, Bonamente M, Mittaz JPD, Durret F, Dos Santos S, Kaastra JS. 1999. *Ap. J.*
Lett. 527:L77
 Lieu R, Mittaz JPD, Bowyer S, Lockman FJ, Hwang CY, Schmitt JHMM. 1996. *Ap.*
J. Lett. 458:L5
 Mastropietro C, Moore B, Mayer L, Stadel J. 2005. *ASP Conf. Ser. Extra-Planar Gas*
 331:89
 Mathur S, Weinberg DH, Chen X. 2003. *Ap. J.* 582:82
 McCammon D, Almy R, Apodaca E, Tiest WB, Cui W, et al. 2002. *Ap. J.* 576:188
 Mulchaey JS. 2000. *Annu. Rev. Astron. Astrophys.* 38:289
 Murali C. 2000. *Ap. J. Lett.* 529:L81
 Murphy EM, Lockman FJ, Laor A, Elvis M. 1996. *Ap. J. Suppl.* 105:369
 Myers AD, Shanks T, Outram PJ, Frith WJ, Wolfendale AW. 2004. *MNRAS* 347:L67
 Nicastro F, Mathur S, Elvis M, Drake J, Fiore F, et al. 2005. *Ap. J.* 629:700
 Nicastro F, Zezas A, Drake J, Elvis M, Fiore F, et al. 2002. *Ap. J.* 573:157
 Oppenheimer BD, Davé R. 2006. *MNRAS* 363:1275
 Penton SV, Stocke JT, Shull JM. 2004. *Ap. J. Suppl.* 152:29
 Persic M, Salucci P. 1992. *MNRAS* 258:14P
 Peterson JR, Kahn SM, Paerels FBS, Kaastra JS, Tamura T, et al. 2003. *Ap. J.* 590:207
 Phillips LA, Ostriker JP, Cen R. 2001. *Ap. J. Lett.* 554:L9
 Pointecouteau E, Arnaud M, Kaastra J, de Plaa J. 2004. *Astron. Astrophys.* 423:33
 Putman ME, Bland-Hawthorn J, Veilleux S, Gibson BK, Freeman KC, Maloney PR.
 2003. *Ap. J.* 597:948
 Rasmussen A, Kahn SM, Paerels F. 2003. *The IGM/Galaxy Connection. The Distribution*
of Baryons at $z = 0$. ASSL Conf Proc. 281:109
 Rasmussen AP, Kahn SM, Paerels F, Willem den Herder J, Kaastra J, de Vries C.
 2007. *Ap. J.* 656:129
 Rasmussen J, Ponman TJ. 2004. *MNRAS* 349:722
 Ravasio M, Tagliaferri G, Pollock AMT, Ghisellini G, Tavecchio F. 2005. *Astron.*
Astrophys. 438:481
 Richter P, Savage BD, Tripp TM, Sembach KR. 2004. *Ap. J. Suppl.* 153:165
 Sanders WT, Lieu D, McCammon D, Rocks L, Vaillancourt JE, et al. 2002. *Bull.*
Am. Astron. Soc. 34:1178

- Sarazin CL, Lieu R. 1998. *Ap. J. Lett.* 494:L177
- Savage BD, Lehner N, Wakker BP, Sembach KR, Tripp TM. 2005. *Ap. J.* 626:776
- Savage BD, Sembach KR, Tripp TM, Richter P. 2002. *Ap. J.* 564:631
- Savage BD, Wakker BP, Fox AJ, Sembach KR. 2005. *Ap. J.* 619:863
- Scharf C, Donahue M, Voit GM, Rosati P, Postman M. 2000. *Ap. J. Lett.* 528:L73
- Schlegel DJ, Finkbeiner DP, Davis M. 1998. *Ap. J.* 500:525
- Sembach KR, Tripp TM, Savage BD, Richter P. 2004. *Ap. J. Suppl.* 155:351
- Sembach KR, Wakker BP, Savage BD, Richter P, Meade M, et al. 2003. *Ap. J. Suppl.* 146:165
- Shull JM. 2003. *The IGM/Galaxy Connection. The Distribution of Baryons at $z = 0$.* ASSL Conf. Proc. 281:1
- Snowden SL, Egger R, Freyberg MJ, McCammon D, Plucinsky PP, et al. 1997. *Ap. J.* 485:125
- Snowden SL, Freyberg MJ, Kuntz KD, Sanders WT. 2000. *Ap. J. Suppl.* 128:171
- Snowden SL, McCammon D, Burrows DN, Mendenhall JA. 1994. *Ap. J.* 424:714
- Soltan AM, Hasinger G, Egger R, Snowden S, Truemper J. 1996. *Astron. Astrophys.* 305:17
- Spergel DN, Bean R, Doré O, Nolta MR, Bennett CL, et al. 2007. *Ap. J.* 170: In press
- Stanimirović S, Dickey JM, Krco M, Brooks AM. 2002. *Ap. J.* 576:773
- Stocke JT, Penton SV, Danforth CW, Shull JM, Tumlinson J, McLin KM. 2006. *Ap. J.* 641:217
- Sunyaev RA, Churazov EM. 1984. *Sov. Astron. Lett.* 10:201
- Taylor JH, Cordes JM. 1993. *Ap. J.* 411:674
- Takei Y, Henry JP, Finoguenov A, Mitsuda K, Tamura T, et al. 2007. *Ap. J.* 655:831
- Takei Y, Ohashi T, Henry JP, Mitsuda K, Fujimoto R, et al. 2007. *Publ. Astron. Soc. Jpn.* 59:339
- Tripp TM, Bowen DV, Sembach KR, Jenkins EB, Savage BD, Richter P. 2006. In *ASP Conf. Proc. 348: Astrophysics in the Far Ultraviolet: Five Years of Discovery with FUSE*, ed. G Sonneborn, H Moos, B-G Andersson, p. 341. San Francisco: ASP
- Tripp TM, Savage BD, Jenkins EB. 2000. *Ap. J. Lett.* 534:L1
- Viel M, Branchini E, Cen R, Ostriker JP, Matarrese S, et al. 2005. *MNRAS* 360:1110
- Voit GM, Evrard AE, Bryan GL. 2001. *Ap. J. Lett.* 548:L123
- Wang QD, Yao Y, Tripp TM, Fang TT, Cui W, et al. 2005. *Ap. J.* 635:386
- Weiner BJ, Williams TB. 1996. *Astron. J.* 111:1156
- Weisskopf MC. 2003. *Adv. Space Res.* 32:2005
- White DA, Fabian AC, Johnstone RM, Mushotzky RF, Arnaud KA. 1991. *MNRAS* 252:72
- Williams RJ, Mathur S, Nicastro F. 2006. *Ap. J.* 645:179
- Williams RJ, Mathur S, Nicastro F, Elvis M. 2006. *Ap. J. Lett.* 642:L95
- Williams RJ, Mathur S, Nicastro F, Elvis M, Drake JJ, et al. 2005. *Ap. J.* 631:856
- Yan M, Sadeghpour HR, Dalgarno A. 1998. *Ap. J.* 496:1044
- Yoshikawa K, Sasaki S. 2006. *PASJ* 58:641
- Zwaan MA, Staveley-Smith L, Koribalski BS, Henning PA, Kilborn VA, et al. 2003. *Astron. J.* 125:2842



Contents

An Accidental Career <i>Geoffrey Burbidge</i>	1
The Beginning of Modern Infrared Astronomy <i>Frank J. Low, G.H. Rieke, and R.D. Gebrz</i>	43
Infrared Detector Arrays for Astronomy <i>G.H. Rieke</i>	77
Heating Hot Atmospheres with Active Galactic Nuclei <i>B.R. McNamara and P.E.J. Nulsen</i>	117
Physical Properties of Wolf-Rayet Stars <i>Paul A. Crowther</i>	177
The Search for the Missing Baryons at Low Redshift <i>Joel N. Bregman</i>	221
Irregular Satellites of the Planets: Products of Capture in the Early Solar System <i>David Jewitt and Nader Haghighipour</i>	261
A New View of the Coupling of the Sun and the Heliosphere <i>Thomas H. Zurbuchen</i>	297
Cold Dark Clouds: The Initial Conditions for Star Formation <i>Edwin A. Bergin and Mario Tafalla</i>	339
Statistical Properties of Exoplanets <i>Stéphane Udry and Nuno C. Santos</i>	397
Relativistic X-Ray Lines from the Inner Accretion Disks Around Black Holes <i>J.M. Miller</i>	441
Toward Understanding Massive Star Formation <i>Hans Zinnecker and Harold W. Yorke</i>	481
Theory of Star Formation <i>Christopher F. McKee and Eve C. Ostriker</i>	565